Chapter 3

Results and Discussion

In this chapter results of characterization of the titanium catalysts derived from different bidentate biphenolate ligands has been presented. The 'biphenols' have been selected by varying their steric bulk as well as by incorporating substitution on the aromatic ring. All these Ti - catalysts have been evaluated for ethylene polymerization and the influence of reaction conditions such as reaction temperature, ethylene pressure, solvent, co-catalyst and Al/Ti ratio on catalytic activity has been examined. In order to have a proper discussion on the nature and structure of catalyst and its performance in ethylene polymerization the chapter has been subdivided in six sections 3.1 to 3.7.

3.1. Ti – BINOLate Catalysts

In this section titanium catalysts derived from C_2 symmetric BINOL, its enantiomers and substituted BINOL have been examined for the polymerization of ethylene.

Catalyst Characterization

The stoichiometric reaction between $Ti(OPr^i)_4$ and rac- H_2BINOL or (*S*) or (*R*)-H_2BINOL ligand in toluene solution afforded dark orange coloured complexes. Both the 1:1 and 1:2 complexes, $[Ti(BINOL)(OPr^i)_2]_2$ (**2**) and $[Ti(BINOL)_2]_n$ (**1,3,4**) are soluble in aromatic solvents but only sparingly so in aliphatic hydrocarbons. Depending on the molar ratio of the starting $Ti(OPr^i)_4$ and the BINOL derivative Ti-complexes with interesting structural features have been isolated previously by Heppert and Walsh, a limited number of which were characterized by X-ray crystal structure analysis [1,2]. For instance catalyst **2** has been shown to exist as a dimer in the solid state as shown below in Scheme 3.1 (b)[3]. On the other hand a trimeric complex was obtained by the reaction of *S*-BINOL and $Ti(OPr^i)_4$ Scheme 3.1 (a).

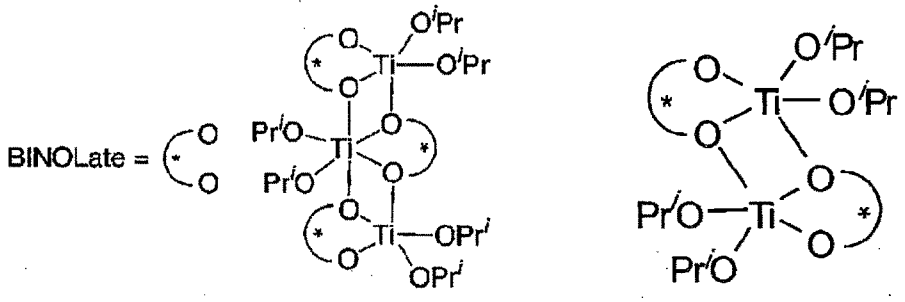

Scheme 3.1 (a) trimeric complex with *S*-BINOL (b) dimeric complex with rac-BINOL.

Catalysts **6** and **7** were isolated as orange coloured microcrystalline powders in moderate yields by reacting $TiCl_4$ or Cp_2TiCl_2 and an equimolar solution of H_2BINOL ligand. Stable complexes of the type Cp_2Ti (O^O) (where O^O = catechol) have previously been isolated employing method (c) [4].

The Ti-BINOLate catalysts have been characterized by microanalysis, ^{1}H NMR, FAB mass spectra and thermal analysis. The ^{1}H NMR spectra was primarily used as a diagnostic tool for ascertaining the purity of complexes (Fig. 3.1). A set of multiplets in the region 7 - 8 ppm for the aromatic protons was a common feature in all cases and in case of **2** additional signals due to methyl protons of *iso* propyl group (1-1.2 ppm) was observed. Traces of starting material H_2BINOL was detected in complex **1** despite repeated washings while purifying the catalyst. The purity was > 90%. In the FAB mass spectra of **1** (Fig.3.2) the parent ion appears at 616 (cal. 617) with low intensity peak for the diol fragment at 286. However, in the case of **2** the parent ion was not detected but the highest observed molecular weight ion at 391 was assigned to Ti(Binol)$(OPr^i)^+$ species which corresponds to parent ion minus coordinated alkoxide. Fragment ions originating from dimeric or trimeric species were difficult to establish due to complexity of the spectrum beyond *m/z* values of 600. Similar band pattern was noted in the EI-MS of other dimeric Titanium alkoxide complexes [5-7]. Thus the exact structure of catalyst **1** in the solid state remains elusive to date.

Recognizing the fact that intra- and intermolecular rearrangement of alkoxide groups in binaphtholate Ti(IV) complexes lead to different structural behavior in solution as well as in solid state we proceeded to examine these catalysts by thermal analysis. We hypothised that the solid state thermal degradation profile might provide some insight

that could help ascertain the composition fixed on the basis of analytical and ^{1}H NMR data. Catalysts **1–7** were heated at a predetermined rate from ambient to 600 °C. In a typical DTA profile (Fig. 3.3) only two major peaks could be seen between 300 – 600°C. Using the percentage wt. loss on the thermogram an attempt was made to assign the possible species corresponding to the observed loss. These results are summarized in Table 3.1. In most cases it was possible to correlate the observed weight loss during thermal decomposition with the empirical formulation. In light of above analytical data and literature facts following structures are proposed in Scheme 3.2.

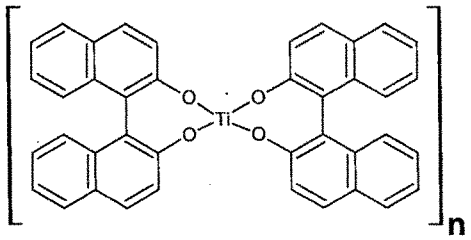

1

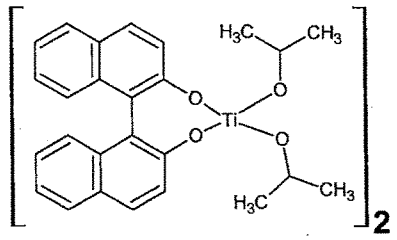

2

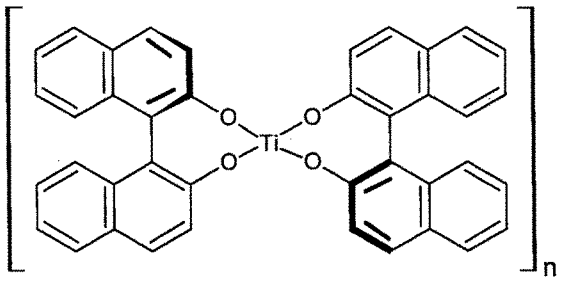

3

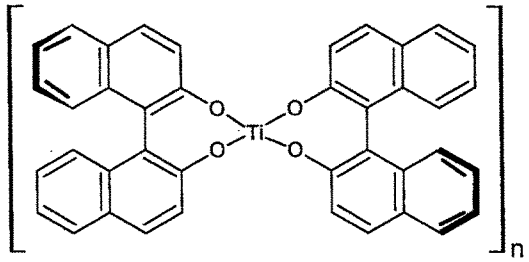

4

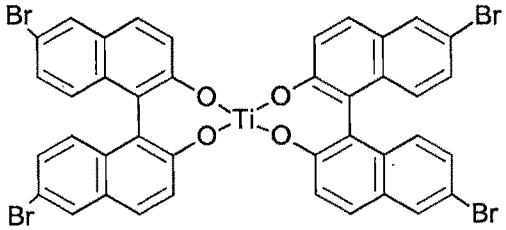

5

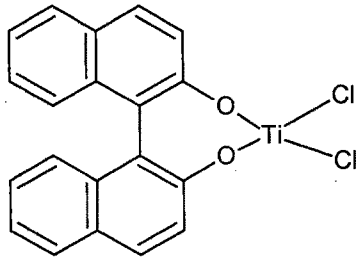

6

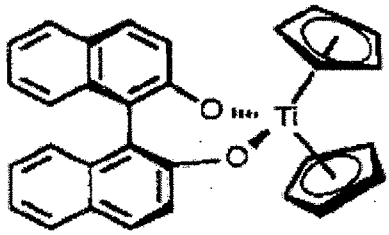

7

Scheme 3.2 Structure of Catalysts **1-7**

Table 3.1 Thermal degradation study of selected catalysts.

Catalyst	M.Wt.	Degradation Temp ° C	% wt. Loss observed	% wt. loss estimated	Fragment assigned
1	616.6	366	21.6	23	naphthyl
		473	56	46	binolate
2	450.5	423	73	76	OPr^i + binol
		437	84	89	TiO_2 (residual)
5	932	375	28	32	2 Br + binol
		433	64	62.8	Br binol
		453	92	94.8	TiO_2 (residual)
6	403	277	47.5	52	2Cl+naphthyl
		346	36.5	35.2	naphthyl
		458	84.2	87.9	TiO_2 (residual)
7	462	315	26.7	28	2Cp
		454	62.0	61.5	binol
		545	88.7	89.5	TiO_2 (residual)

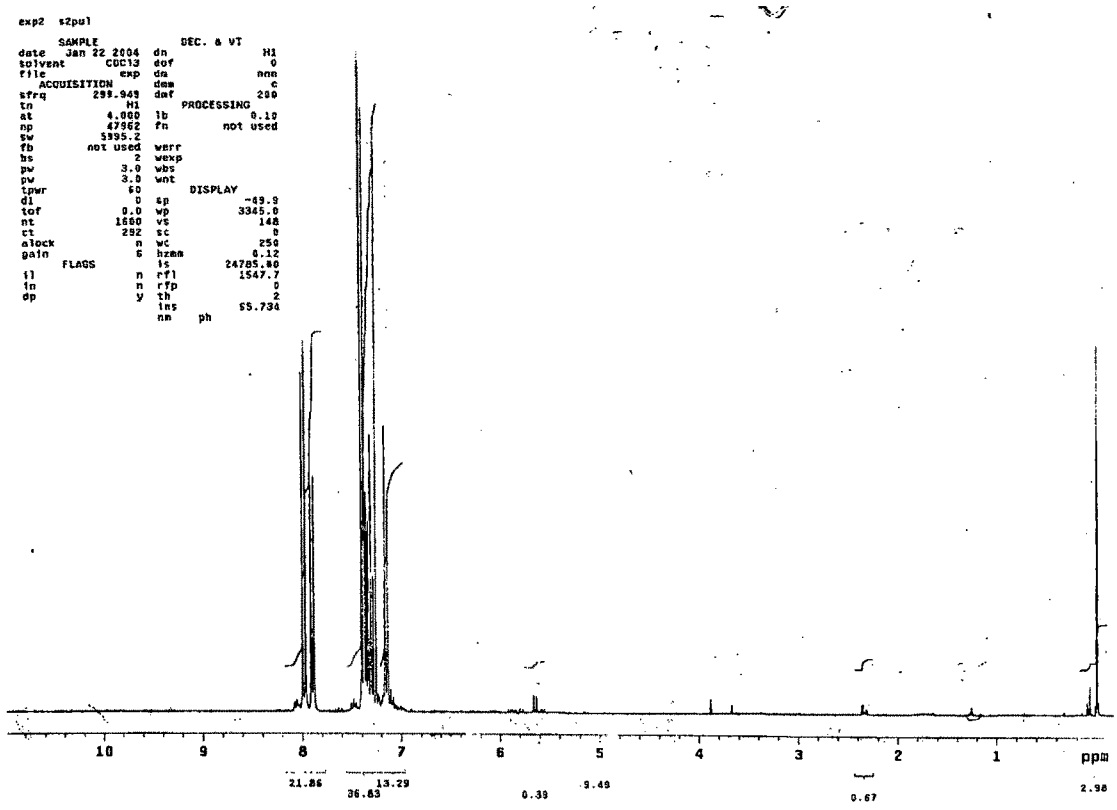

Fig. 3.1. ^{1}H NMR of catalyst 1

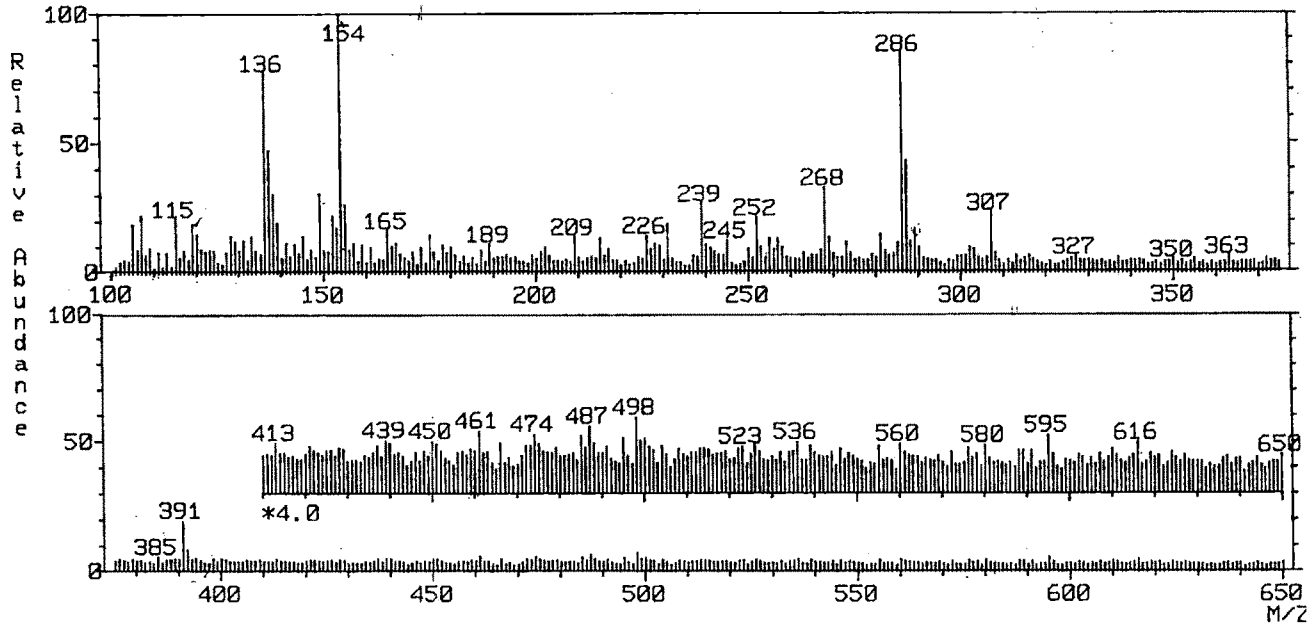

Fig. 3.2 Mass spectra of catalyst **1**

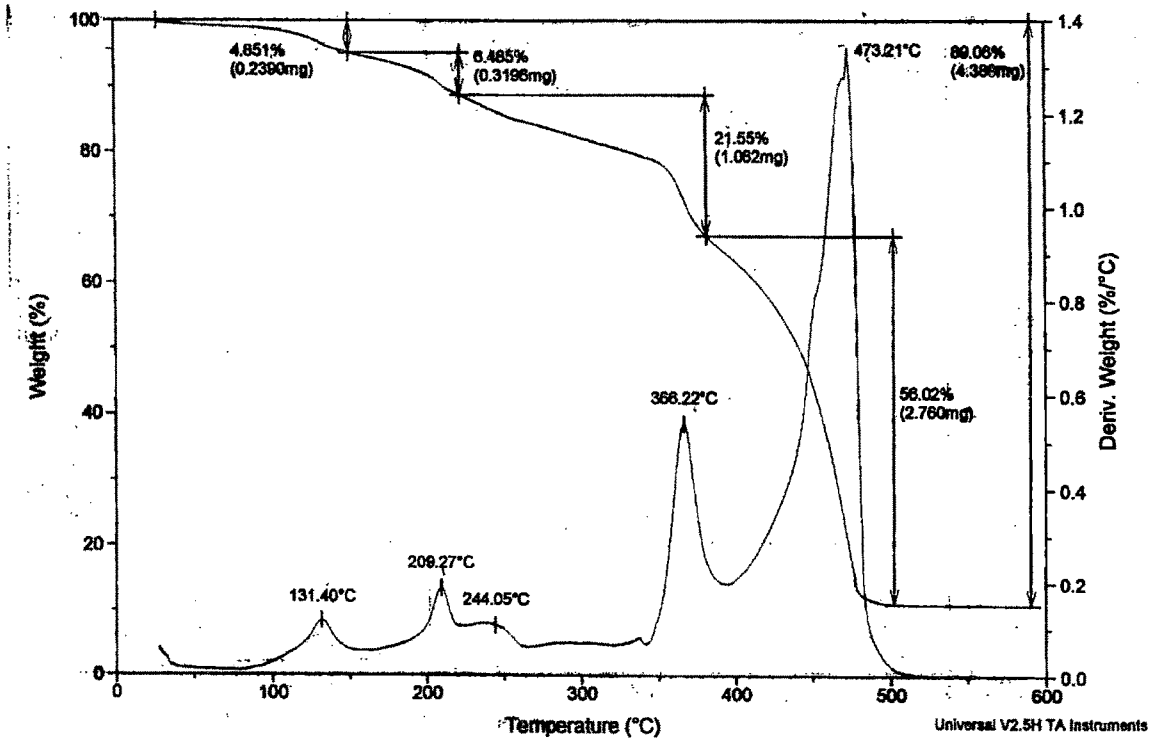

Fig. 3.3. Typical TG/DTA of catalyst **1**

Polymerization of Ethylene

The results of ethylene polymerization using catalyst precursors **1-7** in combination with EASC as co-catalyst are shown in Table 3.2. The efficiency of catalysts was compared with the known metallocene catalysts Cp_2TiCl_2 and Cp_2ZrCl_2. Productivity of the catalysts was studied by varying reaction conditions such as temperature, Al/Ti ratio, pressure, solvent and co-catalysts. Examination of catalyst performance indicate that amongst the different BINOLates, the titanium complexes of Binol derivatives with 1:2 stoichiometry (**1, 3, 4, 5**) display higher activity in polymerization compared to 1:1 complex (**2, 6**). The metallocenes on the other hand are practically inactive under these reaction conditions (entry 8, 9).

The catalytic activity is predominantly dependent on the nature of the co-catalyst (Table 3.3). Ethylaluminum sesquichloride (EASC) displays significantly high polymerization activity. Other chlorinated alkyl aluminums, Et_2AlCl (DEAC) and $EtAlCl_2$ (EADC) are also active but with lowering of productivities. This rather exclusive combination of Ti-BINOLate precursor and EASC co-catalyst in ethylene polymerization suggests formation of specific active intermediates responsible for polymerization. Interestingly amongst the conventional co-catalysts for polyolefin production such as methylalumoxane (MAO) & triethyl aluminum (Et_3Al) only the former shows moderate activity while triethylaluminum is practically inactive.

Detailed studies on the effect of temperature and pressure were then carried out employing complex **1** & EASC as the co-catalyst. From the results summarized in Tables 3.4 & 3.5 it is evident that increasing the reaction temperature from ambient to 100°C has

a marked effect on the activity (Table 3.4, entry 1 & 3). There is over four fold increase of productivity from 2.8 Kg PE /g Ti at R.T. to ~ 12 Kg PE /g Ti at 100°C. The effect of ethylene pressure has been compiled in Table 3.5. Optimum pressure for good activity was around 200 psi at 100°C & Al/Ti ratio of 200 (Table 3.6, entry 2). Surprisingly applying higher pressure under similar conditions does not lead to higher productivity (Table 3.5, entry 4). Interdependence of Al/Ti ratios and temperature has been separately investigated (Table 3.6). Generally a combination of higher Al/Ti ratio and higher temperature lead to improvement in productivity of the catalyst.

A brief examination of effect of different solvents indicated that chlorinated aromatic solvent such as chlorobenzene gave a two fold increase in productivity of polyethylene than that observed for non polar toluene. Ion pairing or ion pair solvation is an important differential factor in single-center polymerization in consonance with earlier study by Deck and Mark [8]. We ascribe that in the present system ion pair reorganization kinetics to be strongly influenced by the solvent. For the polar PhCl ion pair dissociation induces solvent organization and positive entropy. In case of nonpolar solvent such as PhMe ion pair dissociation leads to the usual negative translation and rotation energy terms. Free energy barrier for PhCl may thus be lower than that of PhMe [9]. Similarly aliphatic hydrocarbon solvents such as hexane or heptane resulted in poor activity which may be due to low solubility of catalysts in these solvents.

A noteworthy feature of polyethylene obtained with these Ti-BINOLate catalysts is the invariably low molecular weight (M_w) of the polymer as revealed by GPC analysis. In all cases the PE's display narrow molecular weight distribution (M_w/M_n = 1.8 - 2.6). The bromo-BINOL derivative **5** has nearly similar activity as the unsubstituted

complex **1** but displays higher M_w and melt behaviour. Though the effect of substituted BINOL and its catalytic activity is not very clearly understood at present, it is however pertinent to point out that the monosubstituted tetraaryloxides of titanium such as $Ti(OR)_4$ essentially lead to low molecular weight linear alpha olefins in the C_4-C_{20} carbon range (Schulz-Flory distribution) in sharp contrast to the exclusive formation of solid polyethylene with sterically bulky bidentate $Ti(O\hat{}O)_2$ or $[Ti(O\hat{}O)(OPr^i)]_2$ type complexes employed in the present study [10]. This can be qualitatively interpreted as the rate of chain propogation & termination are nearly equal i.e. $r_p \cong r_t$ in the case of $Ti(OR)_4$-EASC catalyst system resulting in oligomer formation whereas as with $Ti(O\hat{}O)_2$ or $[Ti(O\hat{}O)(OPr^i)]_2$– EASC system $r_p > r_t$ giving polyethylene under identical conditions. The absence of ethylene oligomers in the solution was also confirmed by GC at the end of reaction.

Preliminary study of the reactivity of different olefins towards polymerization with **1**/ EASC were attempted. Interestingly propylene and butene-1 polymerization lead to the formation of low molecular weight liquid oligomers in the slurry. This may be due to the fact that for these higher olefins increase in chain length of the α-olefin may create a barrier for monomer insertion in to the Ti- active BINOLate catalytic species during chain propagation step leading to poor reactivity.

Polyethylene Characterization:

To investigate the properties of polyethylene waxes reported in Table 3.2 they were characterized by GPC (Fig. 3.4). In the GPC a major peak (M_w) centered around 2000 is observed. However, closer examination revealed that in a few cases (b, c and d) a small shoulder appears in the low molecular weight region. This means there might be

more than one type of catalytic species leading to bimodal type of distribution. A commercial PE wax sample was also included as a reference for comparison. GPC of this material also displays similar distribution in the low molecular weight region. An attempt was made to analyze these plots by deconvoluting the GPC. For instance the GPC of sample 'd' was resolved by a PeakFit software and the result is depicted in Fig.3.5. Based on the integration of area under individual peaks it was found that the low molecular weight fraction corresponds to ~ 12 wt% (M_w = 670-700). Surprisingly this fraction does not show any secondary peak in the DSC (T_m). It is possible that this small percentage of low molecular weight fraction does not significantly influence the crystallinity of the wax hence the T_m shows a single sharp melting peak in the region from 80-130°C. As mentioned earlier one of the striking feature of these PE's is the exceptionally low molecular weights (M_w = 1800-3400) and narrow polydispersities (PD = 1.8-2.6). In no case was high molecular weight PE (~ $M_w \geq 10^5$) obtained though these catalysts resemble typical Ziegler systems.

Micronized Polyethylene waxes with interesting applications have similar molecular weights and molecular weight distribution [11]. The DSC (Fig. 3.6) also reveals lower T_m values than that observed for conventional HDPE or LDPE. As a benchmark for comparison of polymer properties with that obtained in this work a known sample of micronized PE-wax was used [11]. The intensity of the equatorial peaks in the X-ray diffractogram (Fig.3.7) for the 110 ($2\theta = 21.6^0$) and 200 ($2\theta = 24^0$) reflection planes for the experimental sample closely match the intensity of the reference sample and the pattern is indicative of orthorhombic crystallinity in these samples. The crystalline nature of these polymers is also supported by the extent of crystallinity

determined from heat of fusion (integration of DSC endotherm) by employing the relationship [12].

$$X_c = H / H_o \times 100$$

Where H = the measured melting enthalpy of the sample

H_o = equilibrium melting enthalpy of 100% crystalline PE = 293 J/g

The X_c thus obtained was in the range of 70-83%.

The polyethylene particles obtained by the above high pressure polymerization are fine and have uniform morphology as seen by Scanning Electron Micrograph. A typical SEM is reproduced in Fig. 3.8. The unique wax like polymer obtained by these Titanium-BINOLate–EASC catalyst system can be fine tuned to tailor the M_w and polydispersities as per requirement of its end use application.

Table 3.2 Ethylene Polymerization with Ti- BINOLate –EASC catalyst system[a]

Entry	Catalyst	Activity Kg PE/g Ti	M_w	PD	T_m °C	d (g/cc)
1	**1**	12	1800	1.8	118	0.963
2	**2**	7	2700	2.6	124	0.955
3	**3**	11	3300	2.6	128	0.952
4	**4**	11	3200	2.5	127	0.955
5	**5**	11	3400	2.4	126	0.954
6	**6**	5	2800	2.2	126	0.960
7	**7**	0.9	--	--	--	0.940
8	Cp_2TiCl_2	0.2	--	--	--	--
9	Cp_2ZrCl_2	0.9	--	--	--	--

[a] All reactions were carried out in a 600 mL SS reactor at 100°C and 200 psi ethylene pressure for 1h in toluene.

Table 3.3 Effect of co-catalysts on ethylene Polymerization at 100 °C

Entry	Co-catalyst[a]	Activity Kg PE/g Ti	T_m °C
1	DEAC	2	125
2	EADC	2.7	--
3	EASC	12	118
4	MAO	1	131
5	TEAL	0.05	--
6	TIBAO	0.6	--

[a]DEAC = Et_2AlCl, EADC = $EtAlCl_2$, TIBAO = tri isobutyl alumoxane

catalyst **1**, $^{p}C_2H_4$ = 200 psi

Table 3.4 Effect of reaction temperature on Polymerization[a]

Entry	Temp °C	Activity Kg PE/g Ti	M_w	PD	T_m °C
1	27	2.8	2200	2.4	129
2	50	3.3	2100	2.6	120
3	100	12	1800	2.0	118

[a]Catalyst **1**-EASC, $^{P}C_2H_4$ = 200 psi.

Table 3.5 Effect of Pressure on Ethylene Polymerization[a]

Entry	$^{P}C_2H_4$ psi	Activity Kg PE/g Ti	M_w	PD	T_m °C
1	100	6	2300	2.4	123
2	200	12	1800	1.8	118
3	300	2.3	2650	2.5	132
4	500	2.2	--	--	--

[a]Catalyst **1**-EASC, Temp = 100 °C

Table 3.6 Influence of Al/Ti ratio and temperature on polymerization[a]

Entry	Al/Ti ratio	Temp °C	Activity Kg PE/g Ti
1	60	100	6.5
2	60	50	2.5
3	200	100	12
4	200	50	4
5	200	27	2.8

[a]Catalyst **1**-EASC, $^{p}C_2H_4 = 200$ psi.

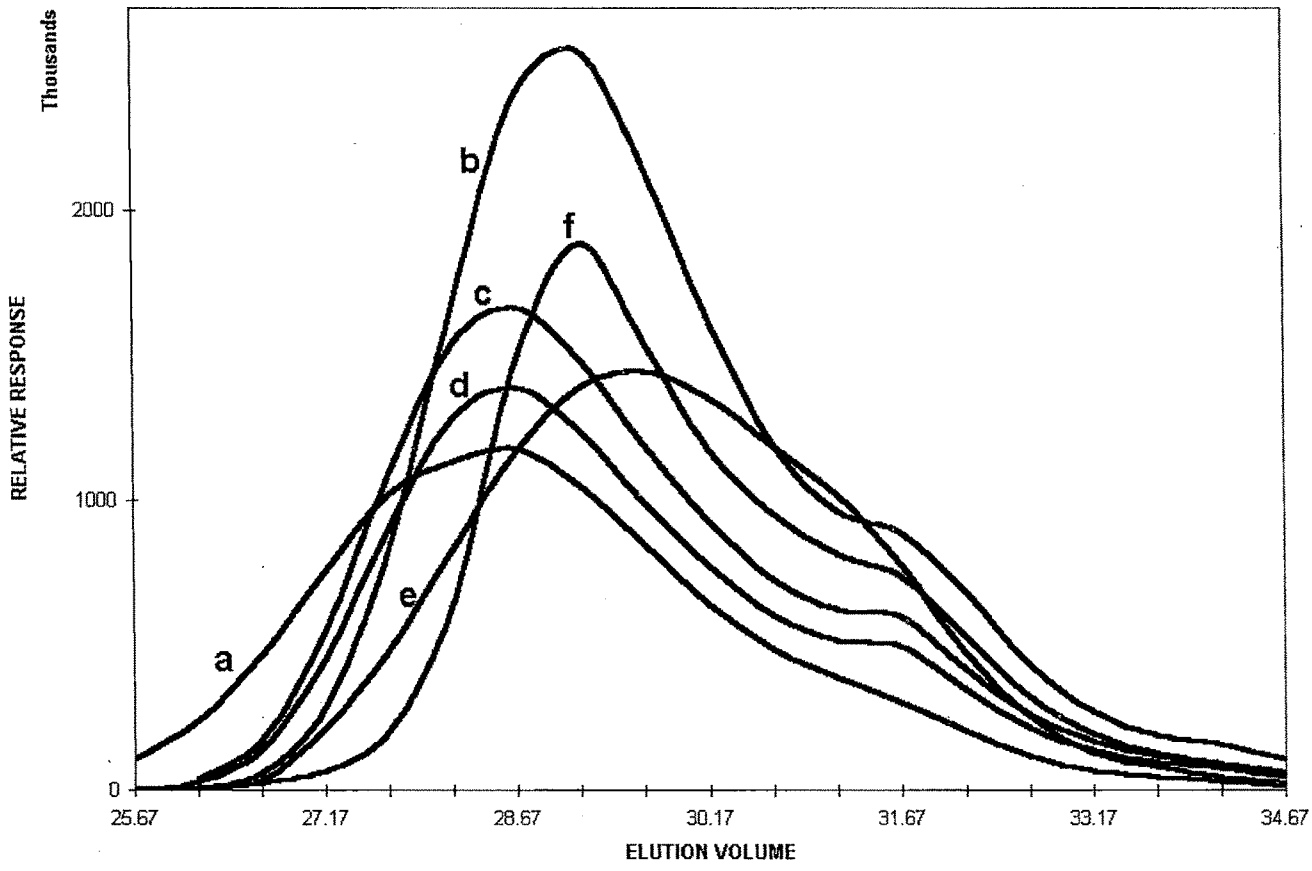

Fig. 3.4. GPC profiles of polymer listed in Table 3.2 a) entry 5, b) entry 2, c) entry 4, d) entry 3, e) entry 1, f) reference sample

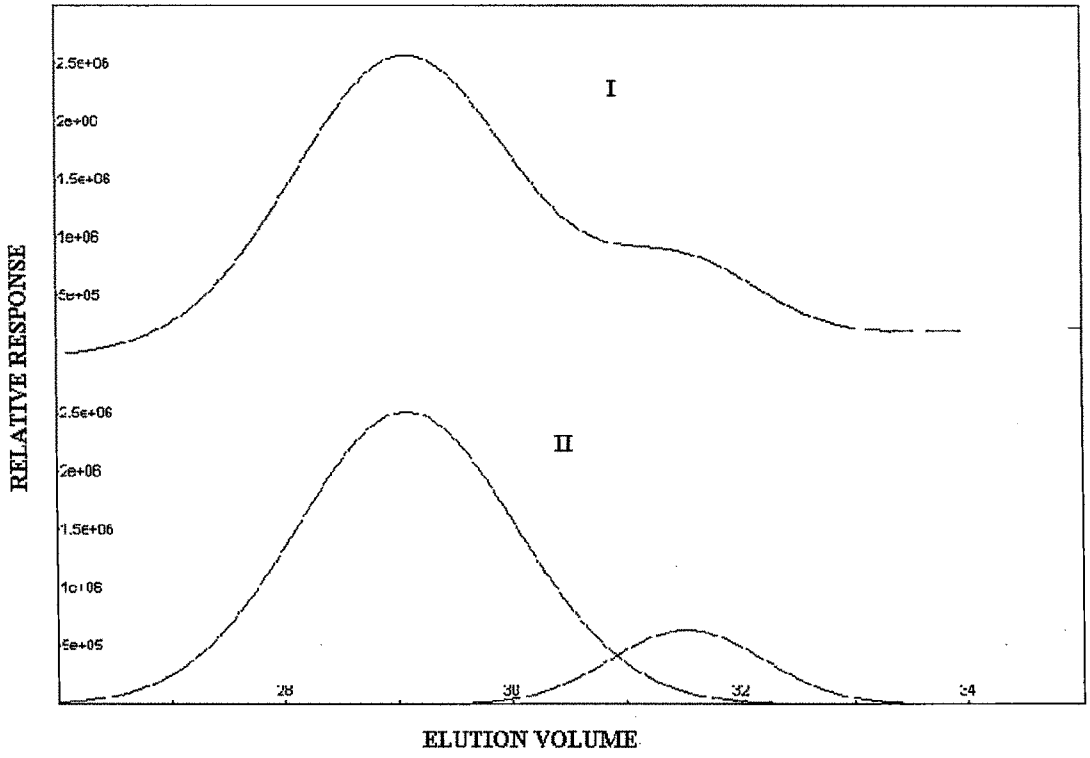

Fig.3.5. Experimental (**I**) and deconvoluted (**II**) GPC trace for a bimodal PE wax (Ref.'d' in Fig. 3.4 ; $r^2 = 0.9893$)

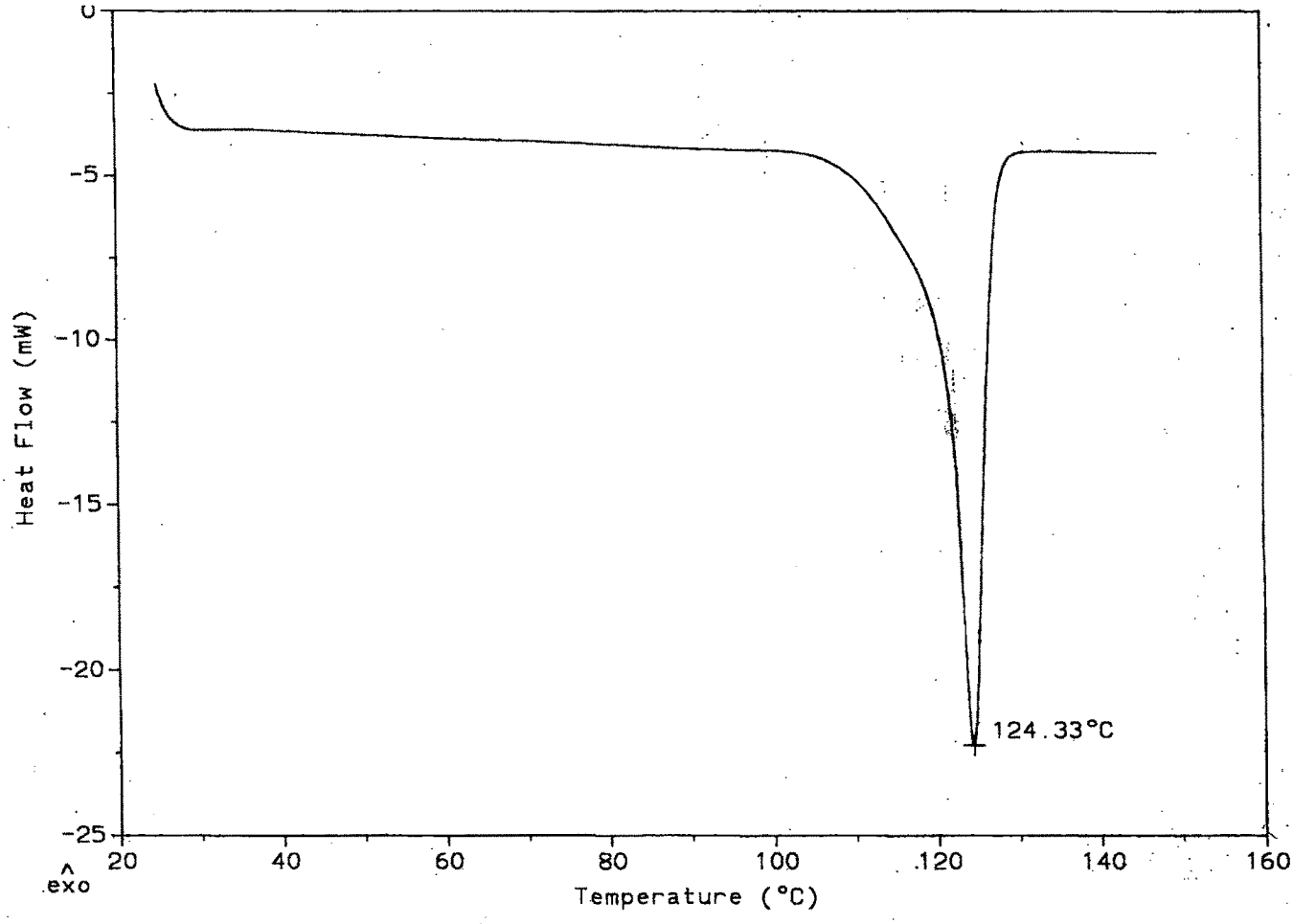

Fig. 3.6. Representative DSC of PE wax sample (Table 3.2, entry 2).

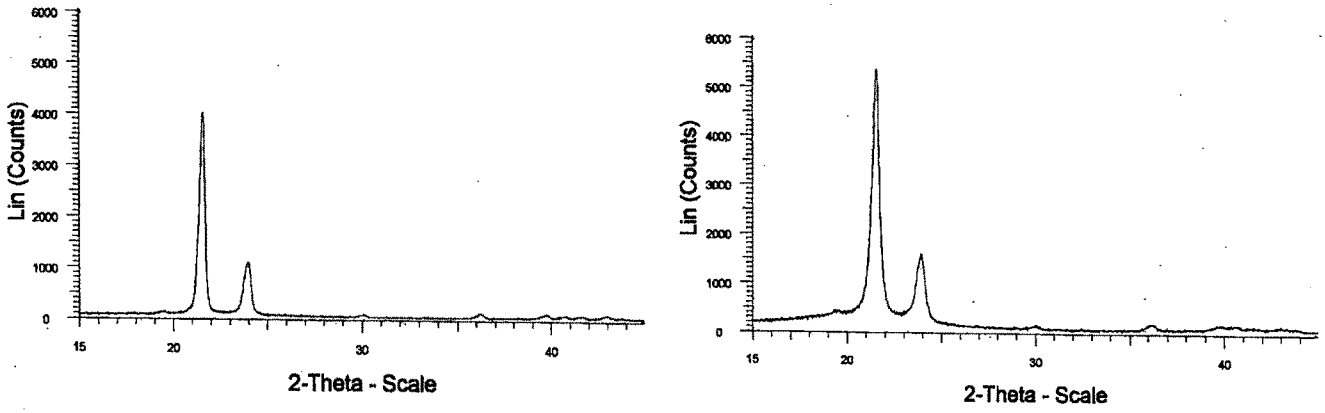

Fig. 3.7. XRD of PE : laboratory sample (left, Table 3.2, entry 1) and Commercial micronised PE sample (right).

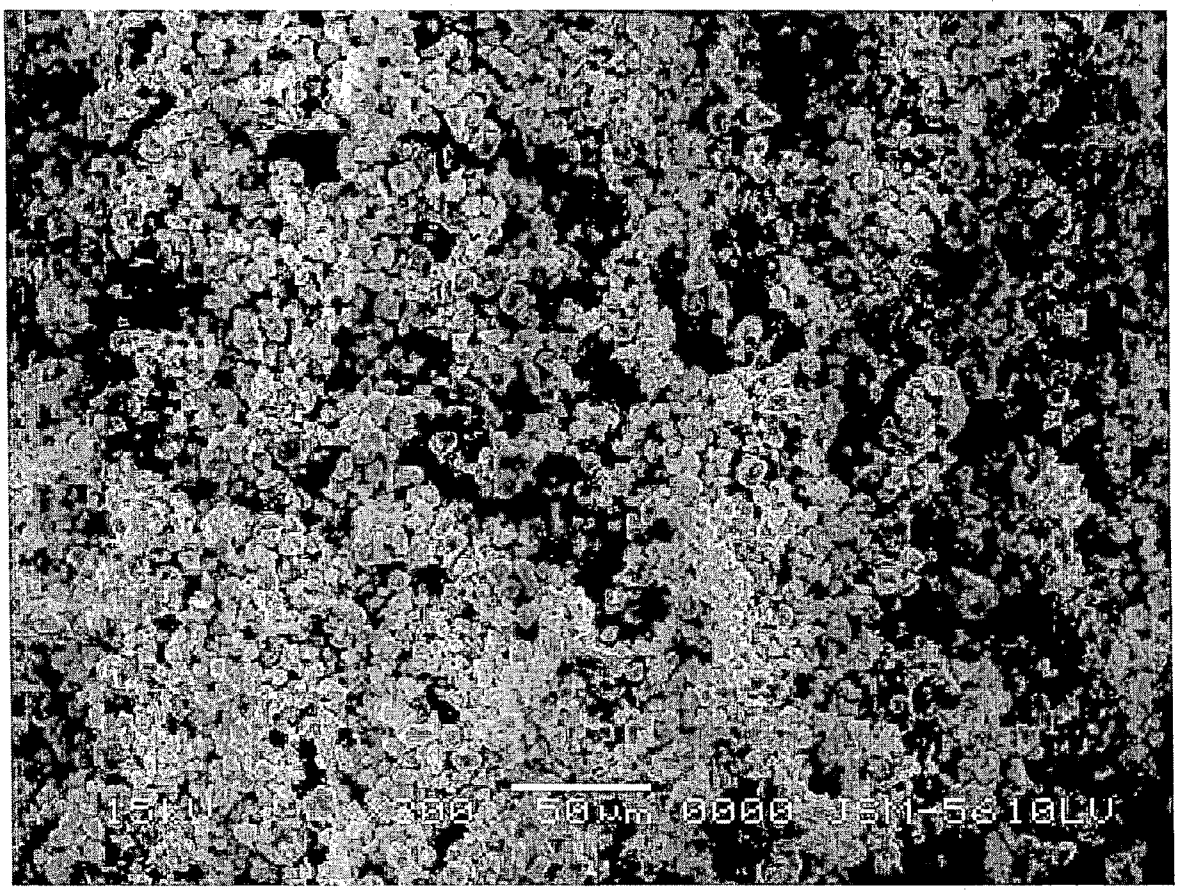

Fig.3.8. SEM of PE wax (Table 3.2, entry 1).

3.2. Ti (di isopropoxy) BIPHENOLate catalysts

In this section complexes of Ti (IV) bearing sterically hindered biphenols such as - biphenol, 1,1'- methylene di-2-naphthol, 2,2'-methylene *bis*(4-chlorophenol), 2,2'-methylene *bis* (6-*tert* butyl-4-ethyl phenol), 2,2' ethylidene *bis* (4,6-di *tert*-butyl phenol) are discussed. The effect of partial substitution of isopropoxide group on ethylene polymerization has been studied. These are thus classified as mixed alkoxo-BIPHENOLate Ti-catalysts.

Catalyst Characterization

The preparation of Ti- BIPHENOLate complexes **(8 – 12)** was accomplished by reacting equimolar quantities of titanium tetraisopropoxide and H_2BIPHENOL ligand. The 1:1 complexes obtained from toluene solutions are dark orange in colour. All the complexes described by the empirical formulation Ti[BIPHENOL$(OPr^i)_2$] are soluble in aromatic solvents but practically insoluble in hexane or heptane.

Chelation of BIPHENOLS

Theoretically the unsubstituted biphenol ligand can bind to the Titanium in at least five different ways as shown in Scheme 3.3. However, the most abundantly formed complexes are those with biphenol in the chelating mode (b) and to a lesser extent, (c) [13].

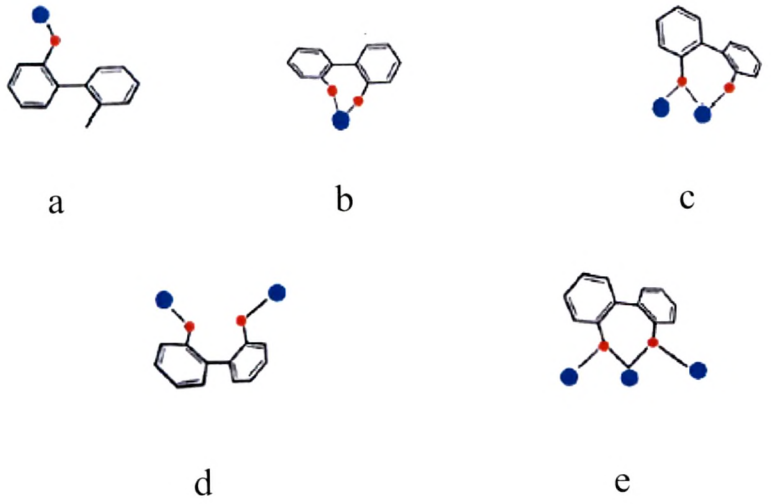

● - **Titanium**

● - **Oxygen**

Scheme 3.3 Coordination modes of the 2,2'-biphenolate ligand : (a) monodentate mode (b) chelate (O,O') mode (c) bridging chelate (O,O,O') mode (d) bridging μ_2-(O,O') mode (e) doubly bridging chelate μ_3 - (O,O,O',O') mode.

In the absence of other ligands, the Lewis acidity of the titanates is enhanced greatly so that coordinative unsaturation is overcome by the formation of aggregates. Depending on the molar ratio of the starting $Ti(OPr^i)_4$ and the biphenol trimeric complexes have been isolated previously and characterized X-ray crystal structure analysis [1, 2] .

Catalysts of the type **8** has been shown to exist as a dimer in the solid state based on X-ray analysis [3]. Thus for catalyst **8** we can envisage that the monomeric $Ti(O\text{-}O)(OPr^i)_2$ can undergo facile inter or intramolecular exchange in solution leading to dimeric forms as indicated by the following equilibria (Scheme 3.4) between the two types of species [14].

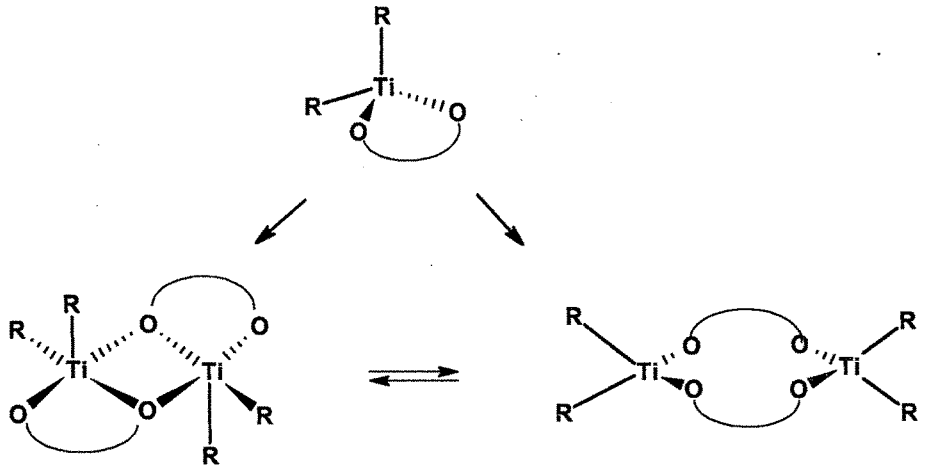

O – O = Biphenol or substituted biphenols, R = OPr^i

Scheme 3.4 Possible solid state equilibria in catalyst **8**

With increasing steric bulk of the biphenolate ligands the tendency to form higher aggregates in the solid state diminishes. Such a phenomena has previously been observed in other Ti-diolate catalysts [15].

The catalysts **8-12** have been characterized by microanalysis, IR, ^{1}H NMR, FAB mass spectra and thermal analysis. Anal calc. for catalyst **8** ($C_{18}H_{22}O_4Ti$); C, 61.7; H, 6.3; Ti, 13.7; Found: C, 60.5; H 6.6; Ti, 13.2. ^{1}H NMR ($CDCl_3$, 300 MHz), 6.96 –7.33 (8H aromatic protons) , 1.16 (12H, CH*Me*$_2$) , 3.97 (2H, *CH*Me$_2$) ; for catalyst **9** ($C_{27}H_{28}O_4Ti$); C, 69.8; H, 6.1; Ti, 10.3; Found: C, 69.2; H 6.1; Ti, 13.0. ^{1}H NMR 6.87 – 7.83 (12H, aromatic protons) , 1.19 (12H, CH*Me*$_2$), 3.91 (2H, *CH*Me$_2$), 4.48 (2H, CH_2 bridge); for catalyst **10** ($C_{19}H_{22}O_4Cl_2Ti$); C, 52.7; H, 5.1; Ti, 11.1; Found: C,53.1; H 5.2; Ti, 11.5. ^{1}H NMR 6.96 –7.23 (6H, aromatic protons) , 1.19 (12H, CH*Me*$_2$), 3.79 (2H, *CH*Me$_2$), 3.92(2H, CH_2 bridge); for catalyst **11** ($C_{31}H_{48}O_4Ti$); C, 69.9; H, 9.1; Ti, 9.0;

Found: C, 69.2; H 9.8; Ti, 9.4. ^{1}H NMR 6.98 –7.24 (4H, aromatic protons) , 1.17 (12H, CH*Me*$_2$), 3.96 (2H, *CH*Me$_2$), 2.56 (4H, *CH*$_2$Me), 1.22 (6H, CH$_2$*Me*), 1.38 (18H, ^{t}Bu); and for catalyst **12** ($C_{36}H_{58}O_4Ti$); C, 71.7; H, 9.7; Ti, 7.9; Found: C,72.1; H 9.3; Ti, 7.6. ^{1}H NMR 7.13 –7.49 (4H, aromatic protons) , 1.18 (12H, CH*Me*$_2$) , 3.50 (2H, *CH*Me$_2$), 4.20 (1H, *CH*Me), 1.67(3H, CH*Me*); 1.38(36H, ^{t}Bu).

In a typical IR spectra of catalyst **8** and the corresponding biphenol the low intensity broad peaks in the 3000-3500 cm^{-1} region indicate deprotonation of the BIPHENOLate ligand.

In the FAB mass spectra of **8** a prominent peak for ligand fragment (biphenolate ion) appears at 186. Again the M^+ parent ion was not detected but the highest observed molecular weight ion at 308 was assigned to Ti(Biphenol)(OPr^i)$^+$ species which corresponds to parent ion minus coordinated alkoxide [1a,16].

In the TG/DTA of these catalyst a single degradation peak around 480^{0}C is indicated which is assigned to the partial loss of bulky biphenol ligand. However, complete degradation to the dioxide, TiO_2 was not noted up to 600^{0}C for this catalyst.

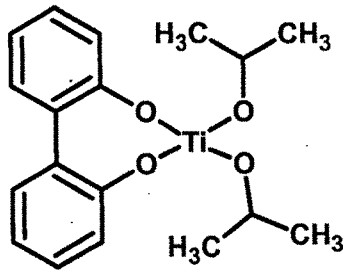

8

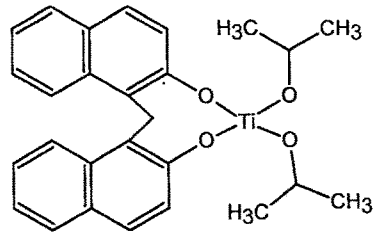

9

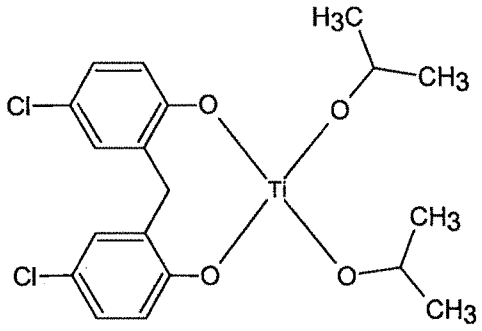

10

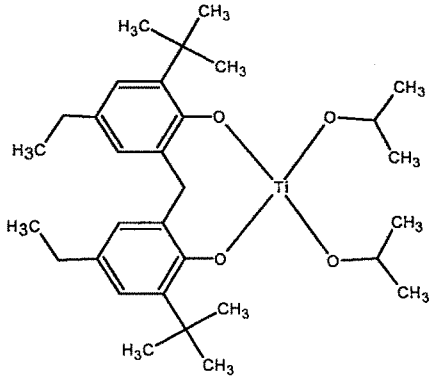

11

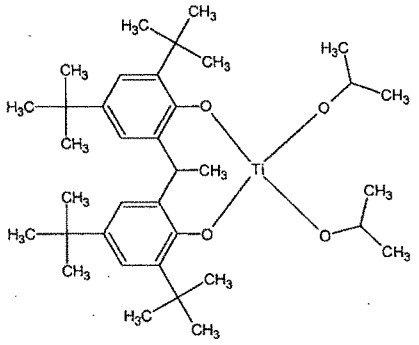

12

Scheme 3.5 Structures of Catalysts **8-12**

Polymerization of Ethylene

The results of ethylene polymerization using catalyst precursors **8-12** are shown in Table 3.7. Experimental data obtained indicate that amongst the different biphenols, the titanium complexes of 2,2'Biphenol (**8**) and ethylidene *bis*-2,4 di- *tert*-butyl phenol (**12**) display higher activity in polymerization. Replacement of phenolic ring with $-CH_2$ linked naphthalene ring leads to lowering of activity (**9**). Reduction in activity was also observed when phenolic ring is substituted by chloro group (**10**) and further reduction on addition of ethyl and *tert*- butyl group (**11**) (Table 3.7, entry 2 and 4). When methyl group is introduced on the CH_2 linkage (**12**) there was pronounced increase in the activity (Table 3.7, entry 5). The effect of substituent in BIPHENOL does not show any definite trend on productivity of PE. Such nonlinear structure activity correlation was not investigated further. Any conclusive correlation between the substitution and the activity towards ethylene polymerization was not observed.

The influence of different Al-alkyl co catalysts was studied (Table 3.8) which reveals that ethylaluminum sesquichloride once again is the most effective cocatalyst for polymerization. Diethylaluminum chloride Et_2AlCl (DEAC) and ethyl aluminum dichloride $EtAlCl_2$ (EADC) are moderately active but methyl alumoxane (MAO) & triethyl aluminum (TEAL, Et_3Al) show poor activity. In the latter case the isolated polyethylene was largely coarse & inhomogeneous.

From the results summarized in Tables 3.9 it is evident that increasing the reaction temperature from ambient to 100°C has marked effect on the activity as seen by about ten-fold increase in polymer yield. (Table 3.9, entry 1 & 3). Further increase in

reaction temperature (140°C) however, shows marginal drop in productivity (entry 4) this may be due to the instability of active species at this temperature.

The effect of ethylene pressure has been compiled in Table 3.10. Increase in ethylene pressure from 300 psi to 500 psi shows higher productivity.

When toluene was replaced by chlorobenzene an increase of ~ 65 % in productivity of polyethylene was observed. Interestingly, this increase is accompanied by a two fold increase in M_w. Aliphatic hydrocarbon solvents such as hexane show poor activity this is ascribed to low solubility of catalyst in this solvent. Polyethylene obtained with these Ti-(di-isopropoxy) BIPHENOLate catalysts have molecular weights (M_w) ranging from 770 to 3380 as revealed by GPC analysis (Fig. 3.9) with narrow polydispersity (M_w / M_n = 1.3 – 1.9). One of the commercial PE wax sample was also included as a reference for comparison [9]. GPC of this material also displays similar distribution in the low molecular weight region. The T_m values in DSC (Fig. 3.10) were between 110.6°C to 129.1°C .

The crystallinity estimated by XRD was in the range 70-83 %. SEM of polymer particles indicate uniform morphology of polyethylene powder..

Table 3.7 : Ethylene Polymerization with $[Ti(O\hat{}O)_2(OPr^i)_2]$–EASC Catalyst System [a]

Entry	Catalyst	Activity Kg PE/g Ti	M_w	PD	T_m °C	d(g/cc)
1	**8**	11.5	1280	1.5	123	0.966
2	**9**	4.0	3380	1.9	129	0.954
3	**10**	8.0	1900	1.7	124	0.955
4	**11**	4.0	770	1.3	110	0.960
5	**12**	11.0	1760	1.5	125	0.953

[a] All reactions were carried out in a 600 mL SS reactor at 100°C and 300 psi ethylene pressure for 1h.

Table 3.8 Effect of aluminum alkyl co-catalysts on Ethylene Polymerization at 100 °C

Entry	Co-catalyst[a]	Activity Kg PE/g Ti	T_m °C
1	EASC	11.5	123
2	DEAC	7.0	127
3	MAO	2.0	132
4	TEAL	1.9	121
5	EADC	3.5	122

[a]DEAC = Et_2AlCl, EADC = $EtAlCl_2$,

Catalyst **8**, $^{P}C_2H_4$ = 300 psi

Table 3.9 Effect of Temperature on Polymerization[a]

Entry	Temp °C	Activity Kg PE/g Ti	T_m °C
1	30	1.0	131
2	60	3.0	128
3	100	11.5	123
4	140	10.0	124

[a]Catalyst **8**- EASC, $^{P}C_2H_4$ = 300 psi.

Table 3.10 Effect of Pressure on Ethylene Polymerization[a]

Entry	$^{P}C_2H_4$ psi	Activity kg PE/g Ti	T_m °C
1	300	11.4	123
2	500	16.5	122

[a] Catalyst **8**-EASC, Temp = 100 °C

Table 3.11 Influence of Solvent on Polymerization[a]

Entry	Solvent	Activity Kg PE/g Ti	M_w	PD	T_m °C
1	Hexane	0.62	--	--	--
2	Toluene	11.5	1280	1.5	123
3	Chloro benzene	19	2520	1.6	121

[a]Catalyst **8**-EASC, $^{P}C_2H_4$ = 300 psi.

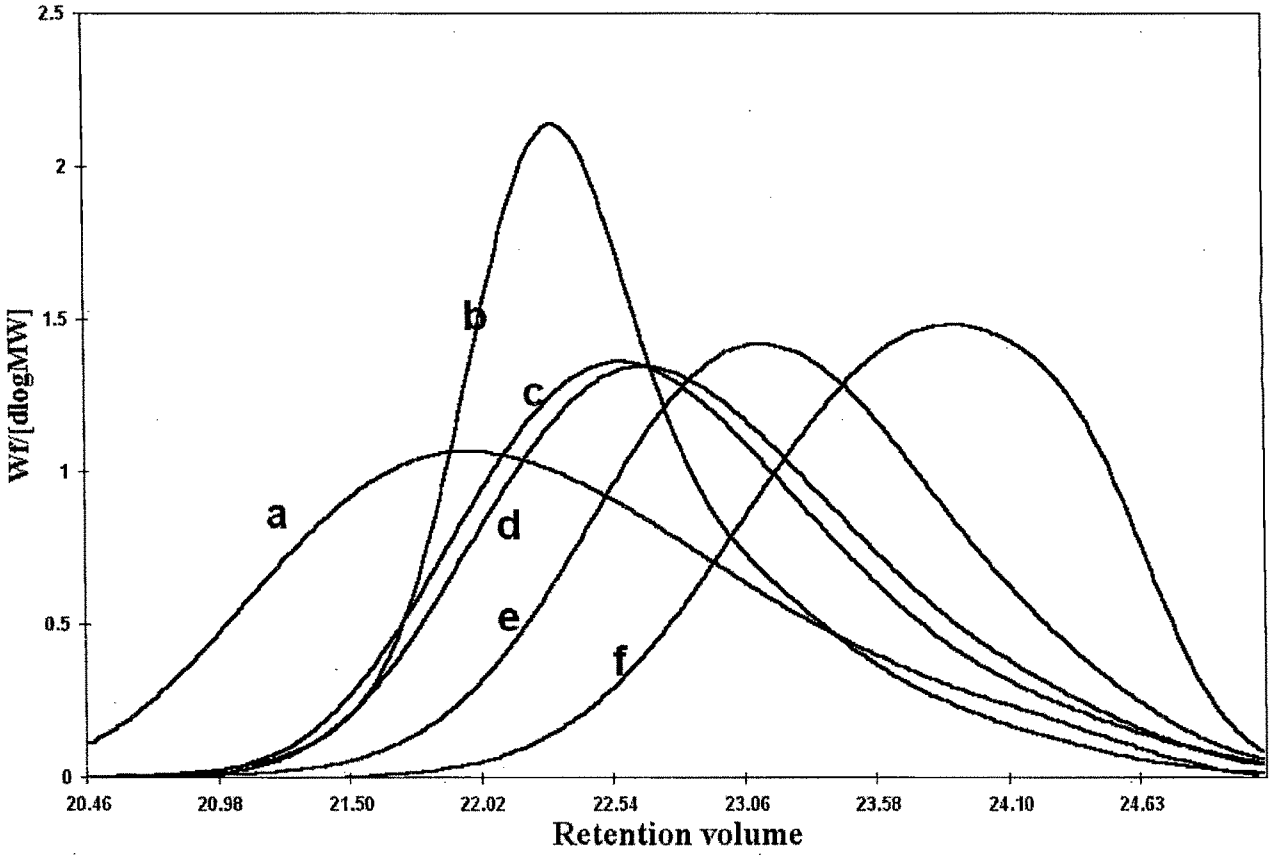

Fig. 3.9 GPC profile of polymer listed in Table 3.7, a) entry 2, b) commercial sample, c) entry 3, d) entry 5, e) entry 1, f) entry 4.

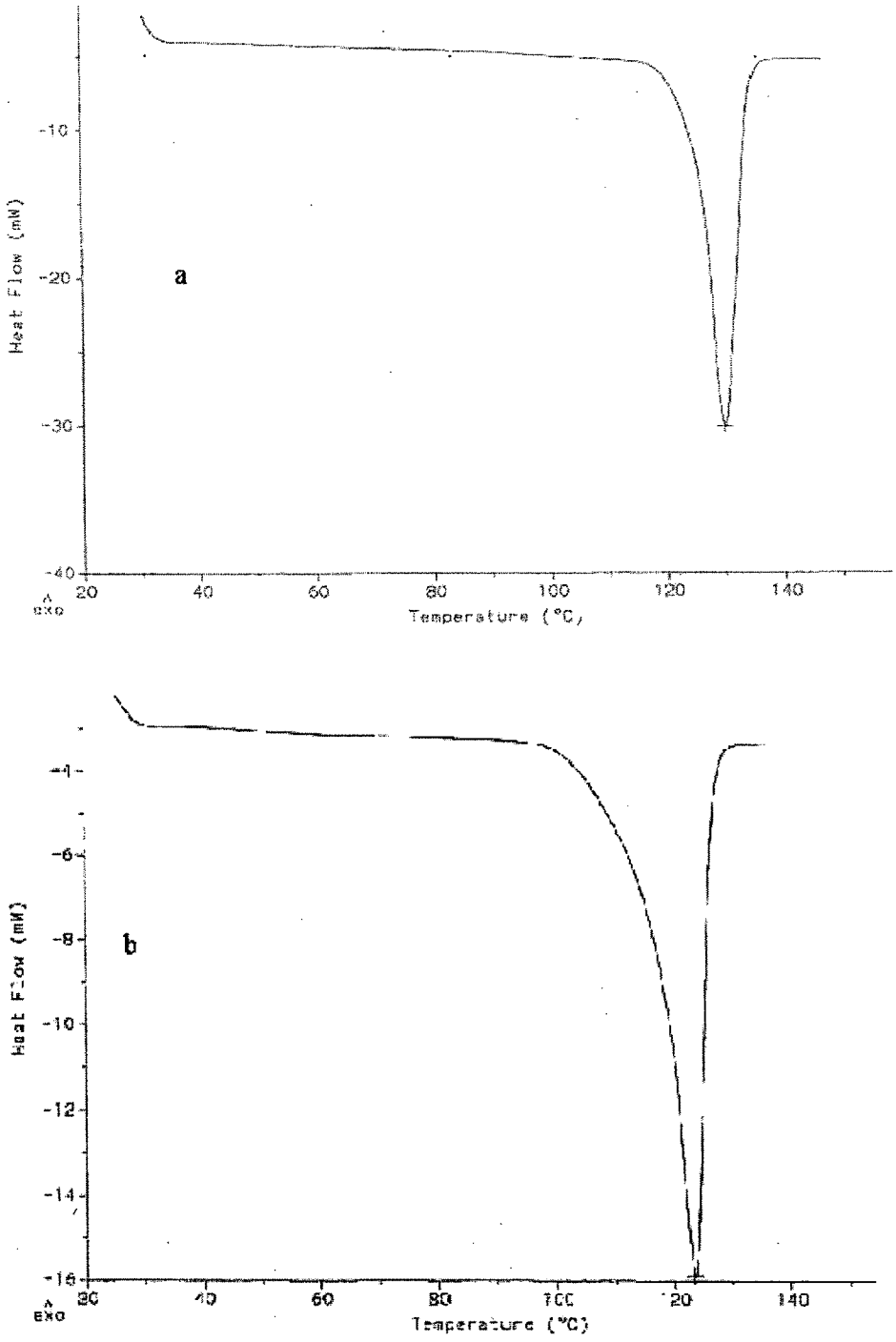

Fig. 3.10 DSC thermogram of PE wax a) commercial sample b) Table 3.7, entry 1

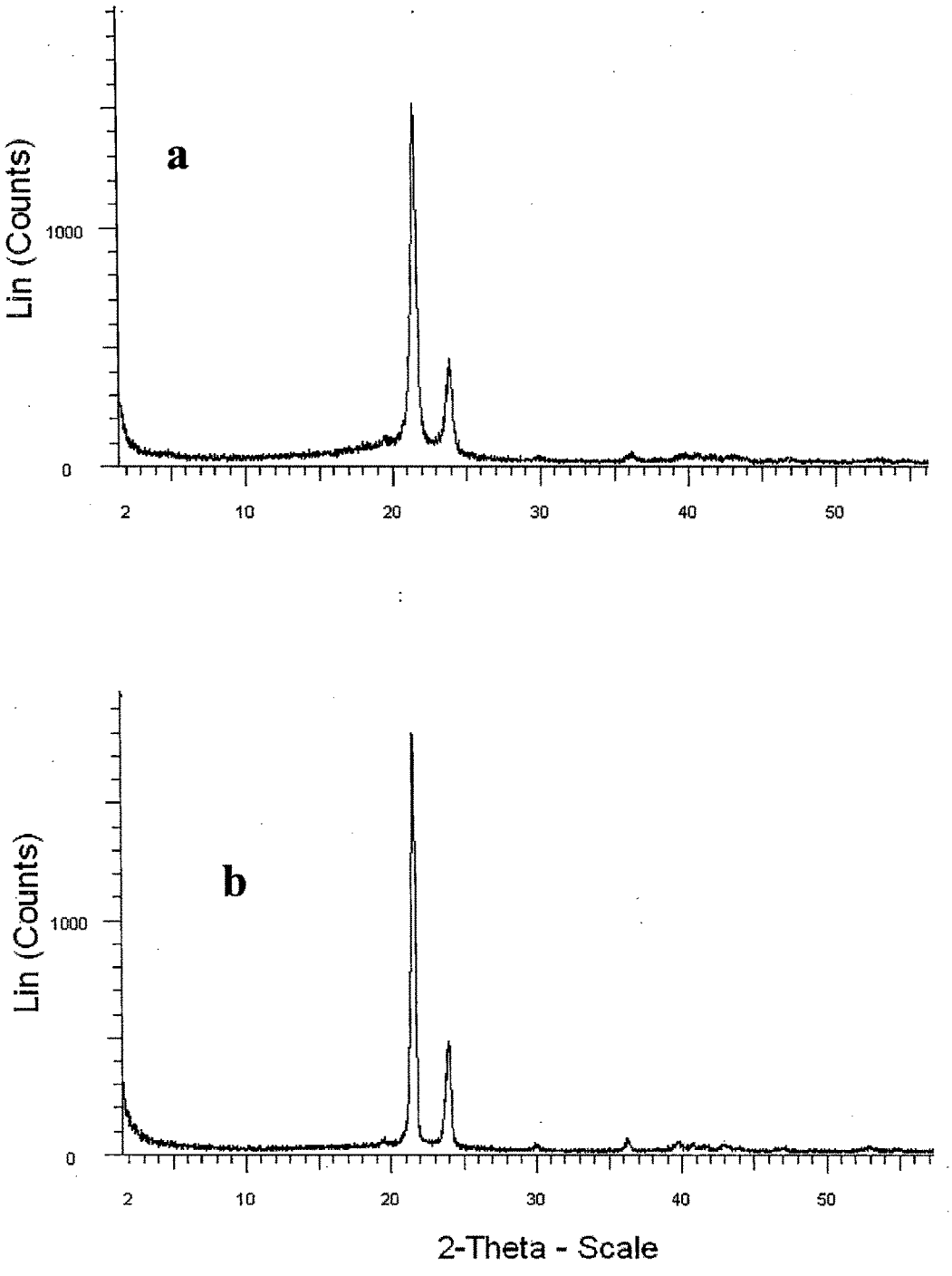

Fig. 3.11 XRD of PE wax (b) (Table 3.7, entry 1) and (a) commercial sample

3.3 Ti(2, 2'methylene*bis* (4-methyl-6-*tert* butyl) phenolate) complexes

In this section 1:1 & 1:2 complexes of Titanium (IV) with sterically bulky ligand 2, 2'methylene*bis* (4-methyl-6-*tert* butyl) phenol (MBP) were synthesized to study the effect of end capped bulky biphenol on catalytic activity.

Catalyst Characterization

Catalyst **13, 14** and **16** were synthesized by adopting the method in literature [17] and confirmed by elemental and NMR analysis. Catalyst **15** was prepared in an analogous manner by stoichiometric reaction using $Ti(OPr^i)_3Cl$ in toluene. The solvent was removed carefully, precipitated solid washed with small amount of warm toluene. Finally orange coloured complex was isolated.

Anal calc. for Catalyst **13** ($C_{29}H_{44}O_4Ti$); C, 69.0; H, 8.8; Ti, 9.5; Found: C, 68.8; H 8.9; Ti, 9.7. ^{1}H NMR (CDCl3, 300 MHz), 6.84-7.25 (4H, aromatic protons) , 1.19 (12H, $CHMe_2$) , 3.88 (2H, $CHMe_2$), 4.56 (2H, CH2 bridging), 18H [$-C(CH_3)_3$], 1.19 (6H Me) ; Catalyst **14** ($C_{46}H_{60}O_4Ti$); C, 76.2; H, 8.3; Ti, 6.6; Found: C,76.4; H 8.3; Ti, 6.7. ^{1}H NMR (CDCl3, 300 MHz), 6.84-7.25 (4H, aromatic protons) , 1.19 (6H, $CHMe_2$) , 3.88 (1H, $CHMe_2$), 4.56 (2H, CH2 bridging), 18H [$-C(CH_3)_3$], 1.19 (6H Me) ;

Catalyst **15** ($C_{26}H_{37}ClO_3Ti$); C, 64.9; H, 7.8; Ti, 9.9; Found: C,65.1; H 7.8; Ti, 10.1. and Catalyst **16** ($C_{23}H_{30}Cl_2O_2Ti$); C, 60.4; H, 6.6; Ti, 10.5; Found: C,60.5; H 6.8; Ti, 10.4 .

The expected M^+ parent ion (505) for **13** was not detected in the FAB mass spectra. A prominent peak for ligand fragment (biphenolate ion) appears at 339-340 along with partial cleavage of ligand was observed at the ion peak position of 163.

The thermal degradation starts only after 290°C. In a typical thermogram of **13** (Fig. 3.12) multiple peaks are observed between 290-480°C suggesting gradual decomposition of ligand fragments which were difficult to quantify. A strong peak around 528^0C is assigned to the complete degradation to the dioxide, TiO_2 (Obs.18.8 %; Cal. 16.0 %) for this catalyst. The titanium estimation *via* gravimetry was generally more accurate for establishing the metal:ligand stoichiometry compared to the analysis by thermal degradation, probably due to improper combustion to TiO_2 in the latter case.

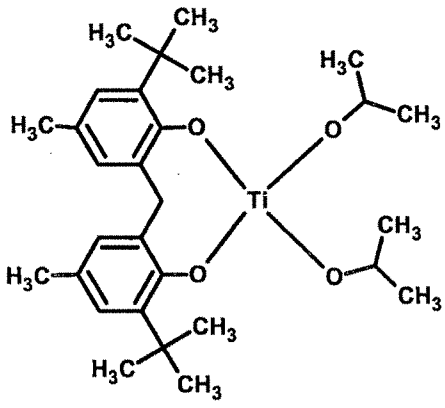

13

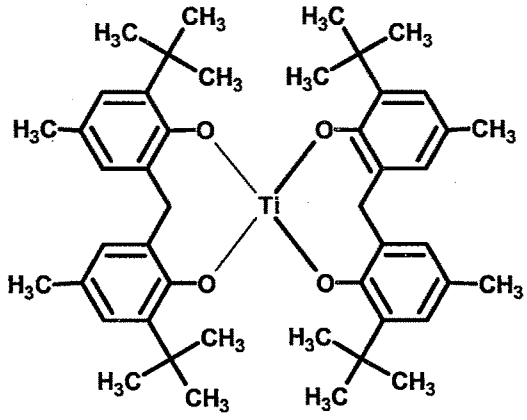

14

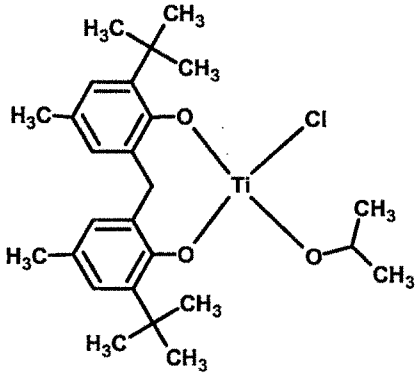

15

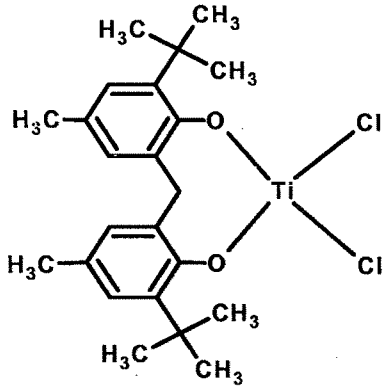

16

Scheme 3.6. Structure of catalyst **13-16**

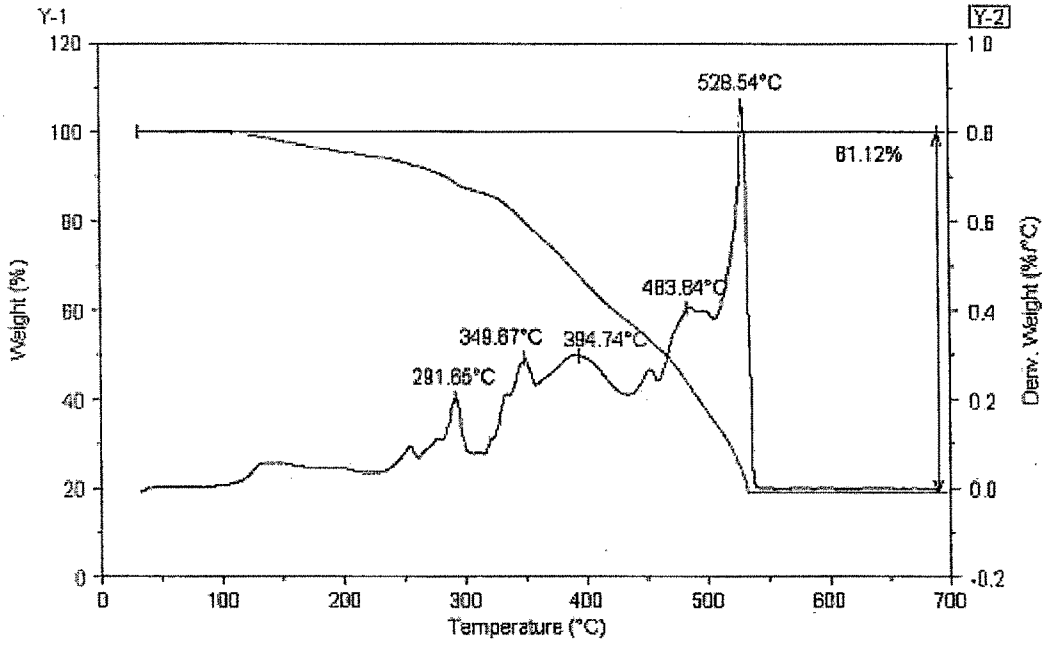

Fig. 3.12 Typical TG/DTA degradation profile of catalyst **13**

Ethylene Polymerization

The results of ethylene polymerization by Ti catalyst based on MBP ligands **13-16** are shown in Table 3.12. Examination of polymerization data indicate that **13** which contains two *iso* propoxy groups shows maximum activity of 11.5 Kg/g of Ti while complete substitution of these pendant groups by chloride (**16**) results in considerable reduction in the polymer yield (2.2 Kg PE/g of Ti). Halide ligands having acceptor properties, polarize Ti-X bonds by imparting partial positive charge to titanium ion. This may facilitate rapid termination of polymer chain which is attributed to strong polarization of neighbouring bonds. Donor alkoxy ligand, on the other hand decreases the positive charge on the titanium ion favouring the four center intermediate formation and olefin insertion in the Ti-C bond.

The efficiency of co-catalysts (Table 3.13) follows the order (EASC) > Et_2AlCl (DEAC) > Et_2AlCl (DEAC).

Increase in the temperature favours the productivity. At 30°C or 60°C catalyst is practically inactive where as at 100°C it increased to 11.4 Kg PE/g of Ti indicating that active species responsible for polymerization forms at high temperature only.

The effect of ethylene pressure has been compiled in Table 3.15 which clearly indicates that higher pressure favours catalytic activity.

Chlorinated solvent such as chlorobenzene showed two fold increase in productivity of polyethylene (22 Kg PE/g Ti) than that for toluene (Table 3.16).

To investigate the molecular properties of polyethylenes further, they were characterized by GPC (Fig. 3.13). Molecular weight was in the range of 750-1630 and

polydispersities 1.4-1.5. The DSC (Fig. 3.15) also reveals lower T_m values 110°C to 117°C.

Branching in PE : In order to characterize the low molecular weight polyethylene obtained in this work, the IR spectra of a standard PE wax sample and that of the low molecular weight polyethylene reported in Table 3.12 were compared.

The branching degree of PEs was determined by taking the value of absorbance of 1378 cm^{-1} peak (ν_{sym} CH_3) [18].

$$\frac{n}{1000C} = \frac{\frac{A_{1378}}{l\rho} - 5.4}{0.691}$$

Where ρ is the density of the polymer in grams per cubic centimeter, *l* is the thickness of the polymer pallet in centimeters As shown in the IR spectrum (Fig.3.14) the reference PE wax sample showed a branching degree of 12 where as PE obtained in this work showed less than 2.

XRD and DSC of PE reveal high degree of crystallinity in the range of 81-86 %. Uniform surface morphology was observed from SEM (Fig. 3.17).

Table 3.12 Ethylene polymerization with Ti(MBP) $(X)_2$–EASC catalyst system [a]

Entry	Catalyst	Activity Kg PE/g Ti	M_w	PD	T_m °C	d*(g/cc)*
1	**13**	11.4	1630	1.42	117	0.955
2	**14**	8.2	1130	1.53	113	0.955
3	**15**	5.8	950	1.47	110	0.956
4	**16**	2.2	750	1.37	111	0.957

[a] Conditions : 600 mL reactor, 100°C, $^{p}C_2H_4$ = 200 psi, t = 1h.

Table 3.13 Effect of co-catalysts on ethylene polymerization at 100 °C[a]

Entry	Co-catalyst[b]	Activity Kg PE/g Ti	T_m °C
1	EASC	11.4	117
2	DEAC	6.1	114
3	MAO	1.4	131
4	EADC	2.7	117
5	TEAL	0.3	--

[a]Catalyst **13**, $^{p}C_2H_4$ = 200 psi

[b]DEAC = Et_2AlCl, EADC = $EtAlCl_2$,

Table 3.14 Effect of temperature on polymerization[a]

Entry	Temp °C	Activity Kg PE/g Ti	T_m °C
1	30	0.2	--
2	60	0.3	--
3	100	11.4	117

[a]Catalyst **13**- EASC, $^{P}C_2H_4$ = 200 psi.

Table 3.15 Effect of pressure on ethylene polymerization[a]

Entry	$^{P}C_2H_4$ psi	Solvent	Activity Kg PE/g Ti	T_m °C
1	100	Toluene	5.4	120
2	200	Toluene	11.4	117
3	500	Toluene	15.5	122

[a] Catalyst **13**-EASC, Temp = 100 °C

Table 3.16 Influence of solvent on ethylene polymerization[a]

Entry	Solvent	Activity Kg PE/g Ti	T_m °C
1	Hexane	0.3	--
2	Toluene	11.4	117
3	Chloro benzene	21.5	122

[a]Catalyst **13**-EASC, $^{P}C_2H_4$ = 200 psi.

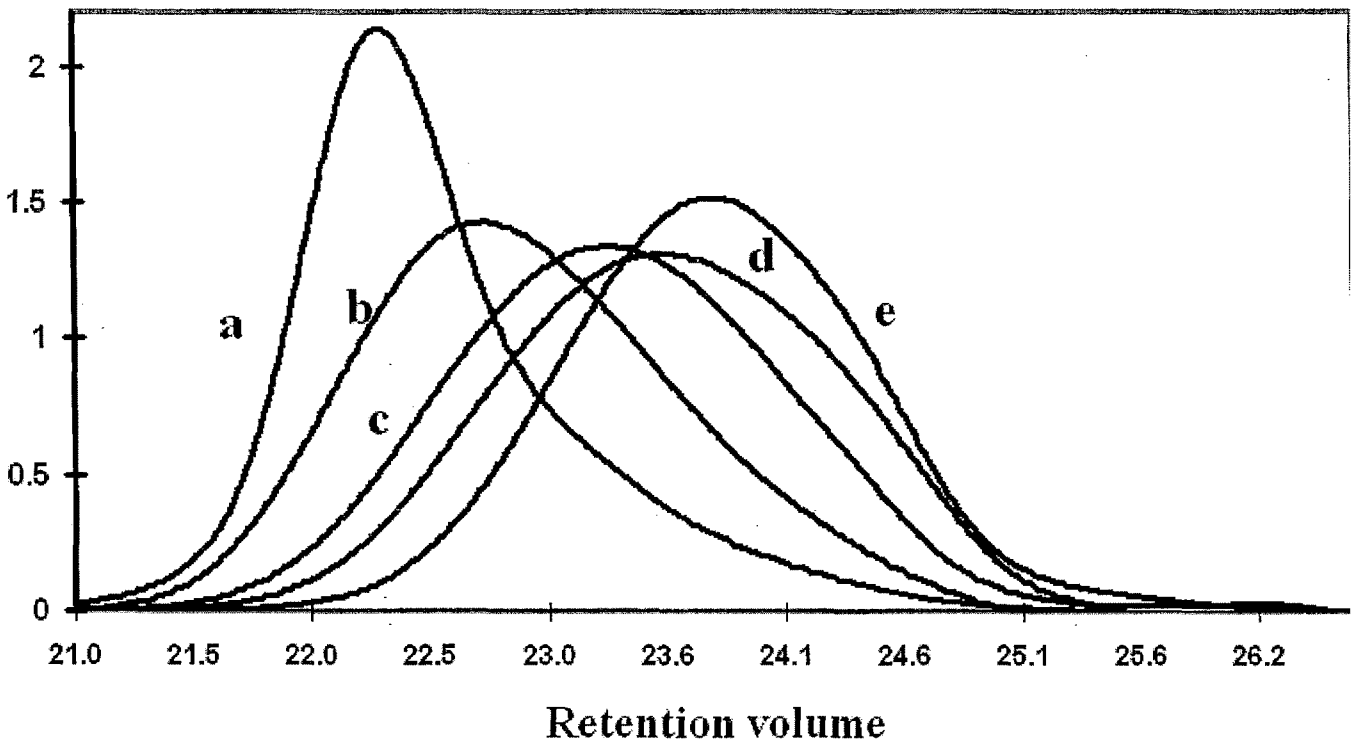

Fig. 3.13. GPC profile of polymer listed in Table 3.12 a) reference sample, b) entry 1, c) entry 2, d) entry 3, e) entry 4.

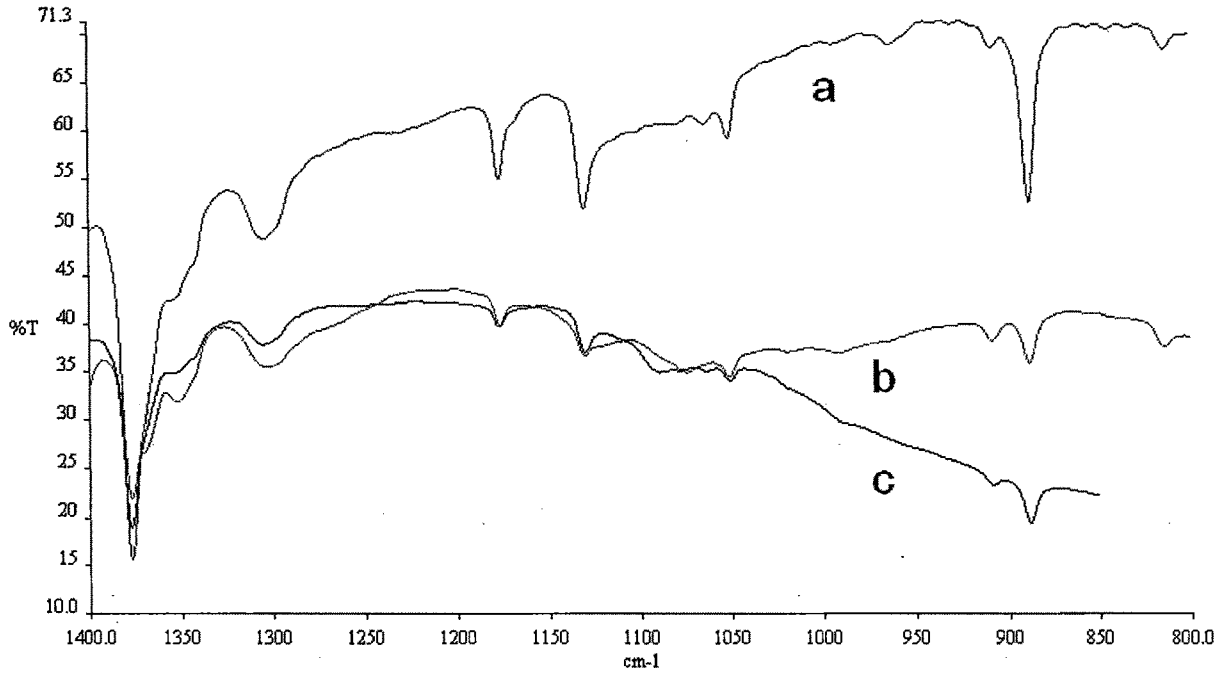

Fig. 3.14 IR spectra for PE sample a) commercial sample b) Table 3.12, entry 1 c) Table 3.12, entry 2.

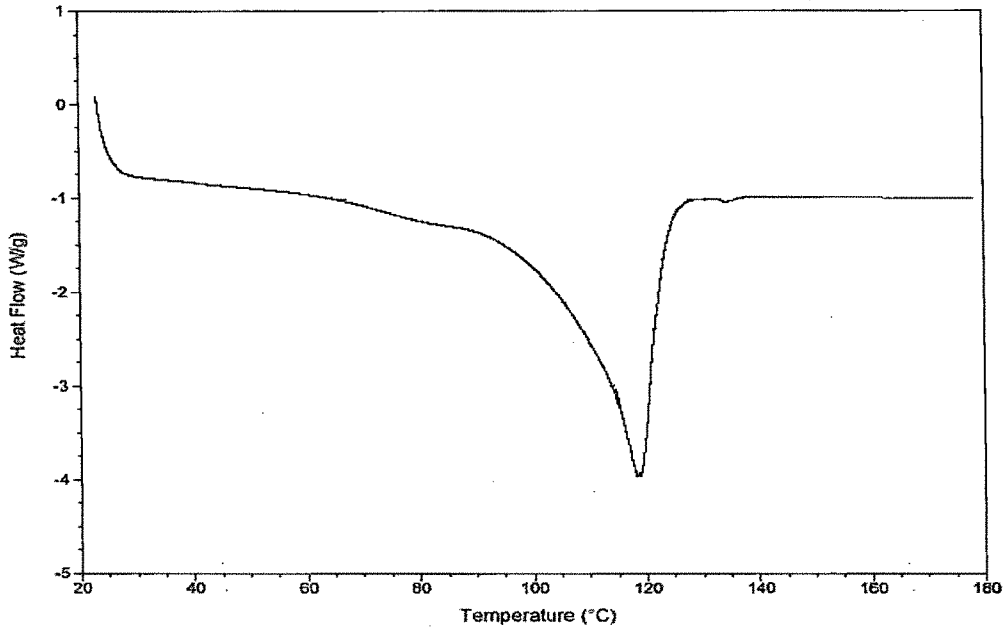

Fig. 3.15 DSC of polymer Table 3.12 entry 1

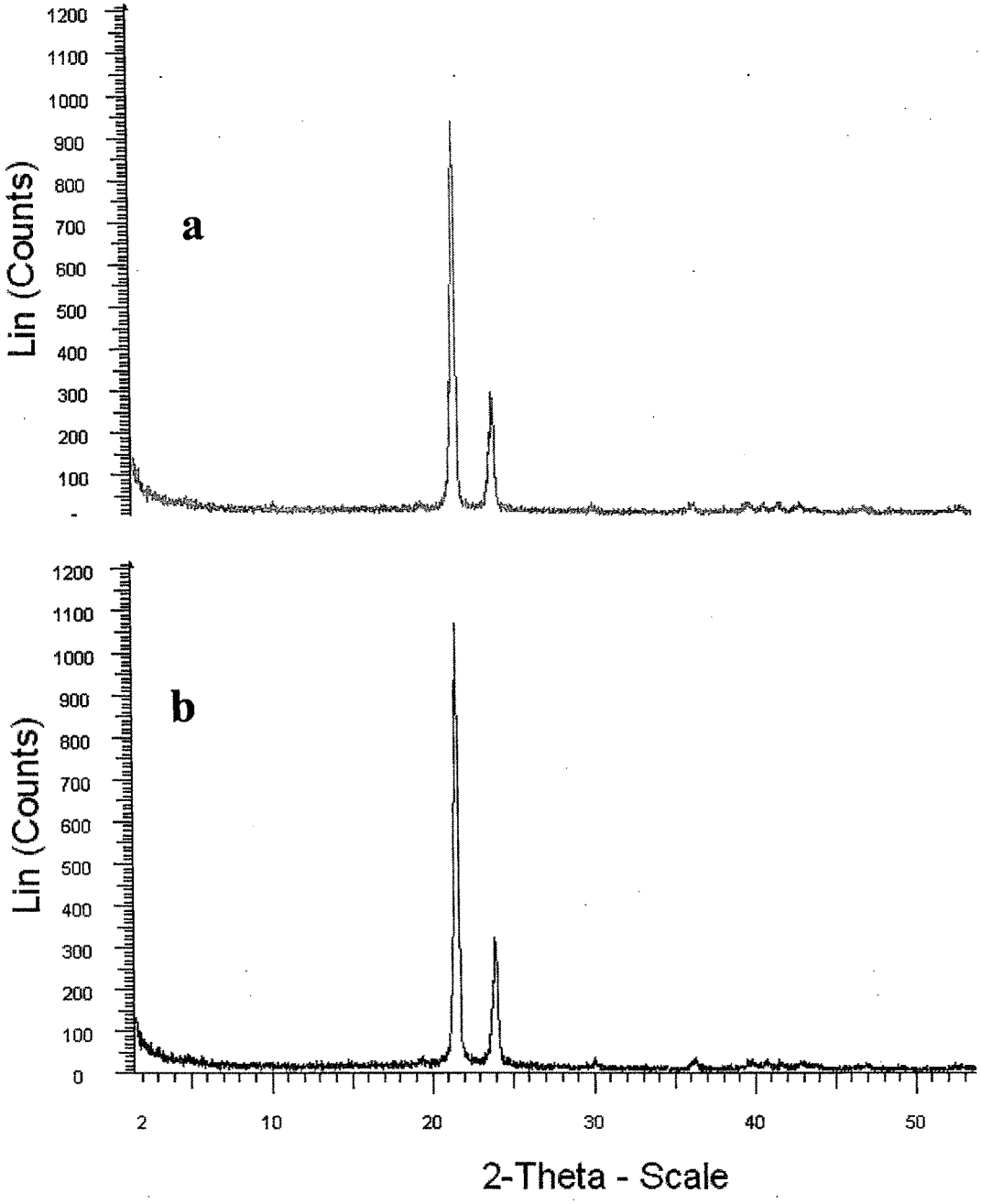

Fig. 3.16. XRD of PE wax table 3.12 (a) entry 1 (b) entry 2

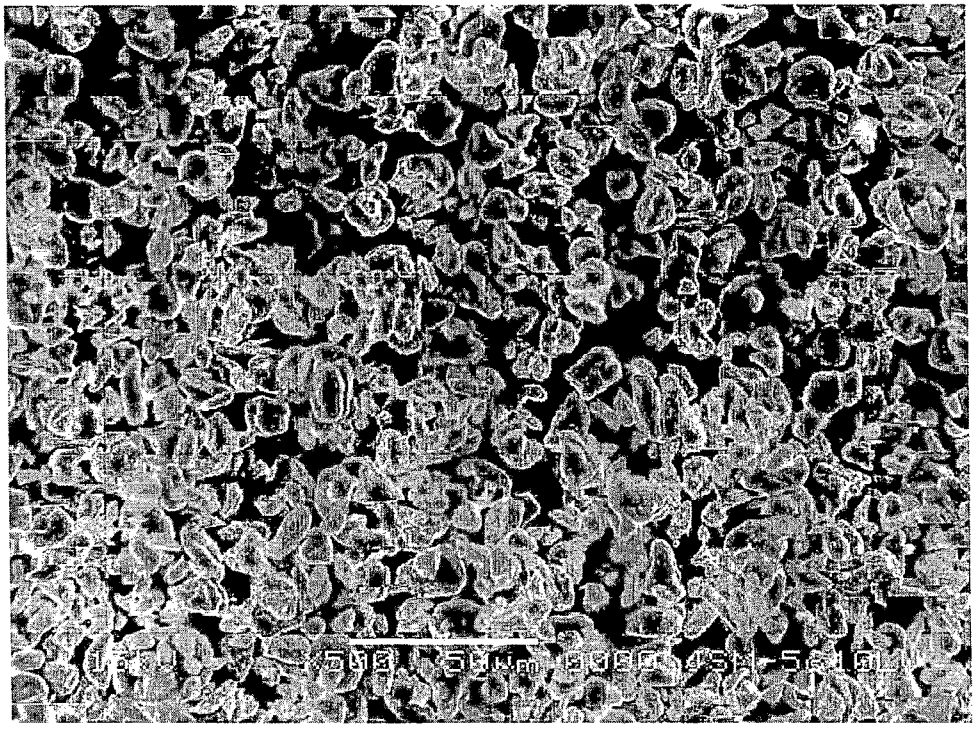

Fig. 3.17 SEM of PE wax Table 3.12, entry 1

3.3. [Ti(O^O)(OPr^i)Cl] Complexes

In this section catalyst precursors formulated as [Ti(O^O)(OPr^i)Cl] (**17-20**) bearing different mono & bidentate phenolic ligands such as phenol, biphenol, 1,1'-binaphthelene 2,2' diol (H_2BINOL) and 1,1'-methylene di-2-naphthol while retaining ancillary groups like isopropoxy and chloride on titanium center have been evaluated for ethylene polymerization.

Catalyst characterization

Catalyst **17** was synthesized by slow addition of 1 mmol (284.3 mg) of $Ti(OPr^i)_3Cl$ in toluene (25 mL) to 1 mmol (284.0 mg) of 1,1' binaphthalene-2,2'-diol (H_2BINOL) in warm toluene (30 mL) under nitrogen atmosphere and heated at 60°C for 3 h. The orange coloured complex was isolated as described in chapter 2. The remaining catalysts **18-20** were prepared in an analogous manner by using the corresponding bi /mono phenol as the case may be. Anal calc.for catalyst **17** ($C_{23}H_{19}O_3ClTi$); C, 64.7; H, 4.5; Ti, 11.22; Found: C, 64.2; H 4.9; Ti, 11.9. ^{1}H NMR ($CDCl_3$, 300 MHz), 7.08-8.82 (12H, aromatic protons), 1.19 (6H, CH*Me*$_2$), 3.88 (1H, *CH*Me$_2$); catalyst **18** ($C_{24}H_{21}O_3ClTi$); C, 65.4; H, 4.8; Ti, 10.9; Found: C,65.7; H 4.6; Ti, 11.1. ^{1}H NMR 7.02-8.76 (12H, aromatic protons), 1.21 (6H, CH*Me*$_2$), 3.49 (1H, *CH*Me$_2$), 4.74 (2H, CH_2 bridge); catalyst **19** ($C_{15}H_{15}O_3ClTi$); C, 55.2; H, 4.6; Ti, 14.7; Found: C,55.3; H 4.9; Ti, 14.4. ^{1}H NMR 7.02-7.35 (8H, aromatic protons), 1.22 (6H, CH*Me*$_2$), 4.04 (1H, *CH*Me$_2$) and catalyst **20** ($C_{15}H_{17}O_3ClTi$); C, 54.8; H, 5.2; Ti, 14.6; Found: C,54.7; H 5.0; Ti, 14.3. ^{1}H NMR 6.82 -7.25 (10H, aromatic protons) , 1.24 (6H, CH*Me*$_2$), 4.10 (1H, *CH*Me$_2$).

The equimolar reaction of $Ti(OPr^i)_3Cl$ and phenolic ligands lead to $Ti(Biphenol)(OPr^i)Cl$ (**18-20**) /$Ti(phenol)_2(OPr^i)Cl$ (**17**). In a typical IR spectra of **17** the low intensity broad peak in the 3000-3500 cm^{-1} region indicate deprotonation of the biphenolate ligand. Other characteristic peaks of **17** and their assignments are (in cm^{-1}): 3487mbr (ν O-H), 3056m (ν_{bph} C-H), 2960m (ν_{as} CH_3), 1595m, 1502s ($\nu_{bph\text{-}Ti}$ C-C), 1463s (δ_{as} CH_3), 1432s, 1263s, 1227s ($\nu_{bph\text{-}Ti}$ C-O), 1147w (Pr^i), 1100s ($\delta_{bph\text{-}Ti}$ C-H), 1006m ($\nu_{PrO\text{-}Ti}$ C-O).

In the FAB mass spectra of **19** a prominent peak for ligand fragment (biphenolate ion) appears at 186. Molecular ion peak at 233 was assigned to species which corresponds to parent ion minus coordinated alkoxide and chloride. However, the parent ion was not detected.

Thermogram of **19** indicates the thermal stability upto 380^0C. Further increase in temperature indicates partial loss of biphenol ligand (Obs. 39 %; Cal. 43 %). However, complete degradation to the dioxide, TiO_2 was observed beyond 450°C (Obs. 28 %; Cal. 25 %) for this catalyst.

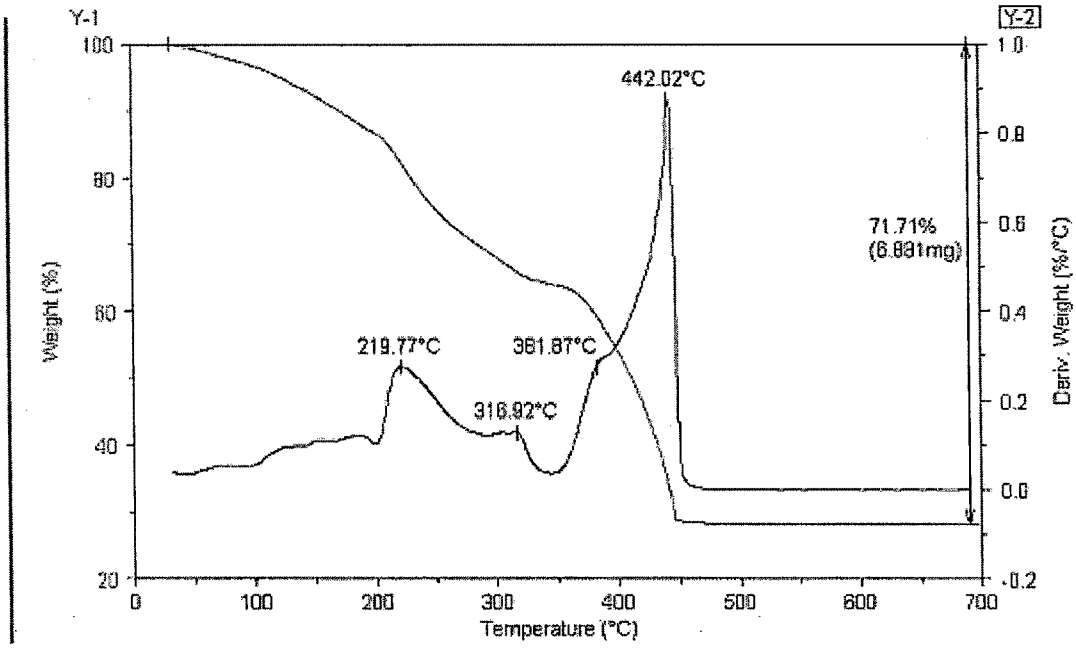

Fig. 3.18 TG/DTA of catalyst **17**.

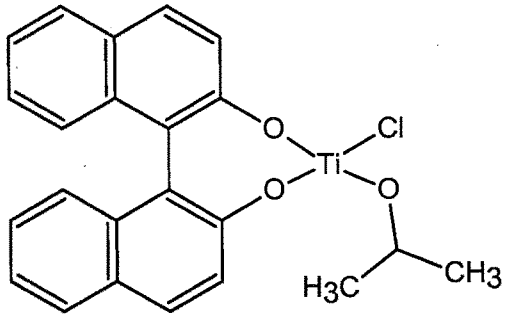

17

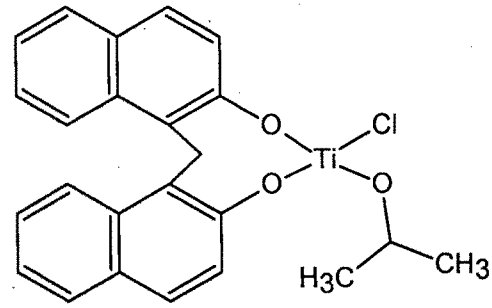

18

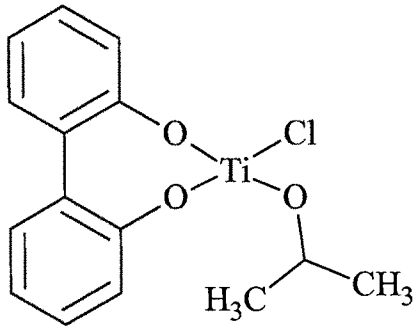

19

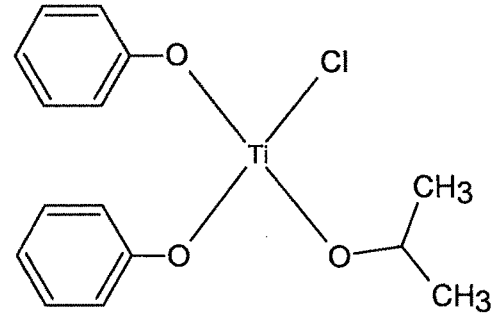

20

Scheme 3.7 Catalyst structure of **17-20**

Polymerization of Ethylene

The results of ethylene polymerization using catalyst precursors **17-20** are shown in Table 3.17. The productivity of catalysts indicate that amongst the different biphenols, titanium complex of H_2BINOL gives the highest productivity (10 KgPE/g Ti) where as the one containing simple phenolic group (**20**) gives low yield (4 KgPE/g Ti). In general it is found that productivity as well the molecular weight of the polymer reduces with reduction in the aromatic ring size.

Table 3.18 indicates that the co-catalyst ethylaluminum sesquichloride gives highest productivity whereas use of Et_2AlCl (DEAC) and $EtAlCl_2$ (EADC) lower the productivities. Conventional co-catalysts methyl alumoxane (MAO) & triethylaluminum (TEAL, Et_3Al) display poor activity.

From the results summarized in Table 3.19 it is clear that increasing the reaction temperature from about 27°C to 100°C has pronounced effect on the activity as seen by about manifold increase in polymer yield.

The effect of ethylene pressure on the productivity has been compiled in Table 3.20. Applying higher ethylene pressure leads to higher productivity irrespective of the solvent. It is also observed that increase in the pressure also lead to the increase in the molecular weight of the polymer as well as melting temperature.

Data of Table 3.21 reveals that chlorobenzene showed ~30 % increase in productivity of polyethylene (12.5 Kg PE/g Ti) than that for toluene (10 Kg PE/g Ti) with slight increase in M_w.

Molecular weight of the PE as obtained by GPC analysis (Fig. 3.19, 3.20) reveals that M_w fall in the range of 840 to 1290 with the narrow PD (M_w / M_n = 1.4-1.5). The

DSC (Fig. 3.21) analysis indicates that the T_m values obtained from DSC are in the range of 105 to 119°C. The crystalline nature of these polymers was estimated by integration of the XRD (Fig 3.22) peaks. High degree of crystallinity is indicated in all cases which was in the range of 80-88 %. Scanning Electron Micrograph of the polymer indicates uniform morphology.

Table 3.17 Ethylene polymerization with Ti-biphenolate –EASC catalyst system [a]

Entry	Catalyst	Activity Kg PE/g Ti	M_w	PD	T_m °C	d(g/cc)
1	17	9.5	1245	1.3	118	0.956
2	**18**	7.2	1200	1.5	119	0.954
3	**19**	5.2	1015	1.6	110	0.955
4	**20**	4.2	910	1.5	105	0.958

[a] All reactions were carried out in a 600 mL SS reactor at 100°C and 300 psi ethylene pressure for 1h.

Table 3.18 Effect of co-catalysts on ethylene polymerization at 100 °C[a]

Entry	Co-catalyst[b]	Activity Kg PE/g Ti	T_m °C
1	EASC	9.5	118
2	DEAC	6.7	113
3	MAO	2.1	136
4	EDAC	1.8	125
5	TEAL	0.2	--

[a]Catalyst **17**, $^{p}C_2H_4 = 300$ psi

[b]DEAC = Et_2AlCl, EADC = $EtAlCl_2$,

Table 3.19 Effect of temperature on polymerization[a]

Entry	Temp °C	Activity Kg PE/g Ti	T_m °C
1	30	0.4	--
2	60	2.3	128
3	100	9.5	118

[a]Catalyst **17**- EASC, $^{p}C_2H_4$ = 300 psi.

Table 3.20 Effect of pressure on ethylene polymerization[a]

Entry	$^{p}C_2H_4$ (psi)	Solvent	Activity Kg PE/g Ti	M_w	PD	T_m °C
1	100	Toluene	3.5	890	1.3	111
2	300	Toluene	9.5	1245	1.5	118
3	500	Toluene	18.3	3200	1.6	119
4	300	Chloro benzene	12.4	1450	1.6	117
5	500	Chloro benzene	24.7	2110	1.7	120

[a] Catalyst **17**-EASC, Temp = 100 °C

Table 3.21 Influence of solvent on polymerization[a]

Entry	Solvent	Activity Kg PE/g Ti	M_w	PD	T_m °C
1	Hexane	0.8	--	--	--
2	Toluene	9.5	1245	1.5	118
3	Chlorobenzene	12.5	1550	1.6	117

[a]Catalyst **17**-EASC, $^{p}C_2H_4 = 300$ psi.

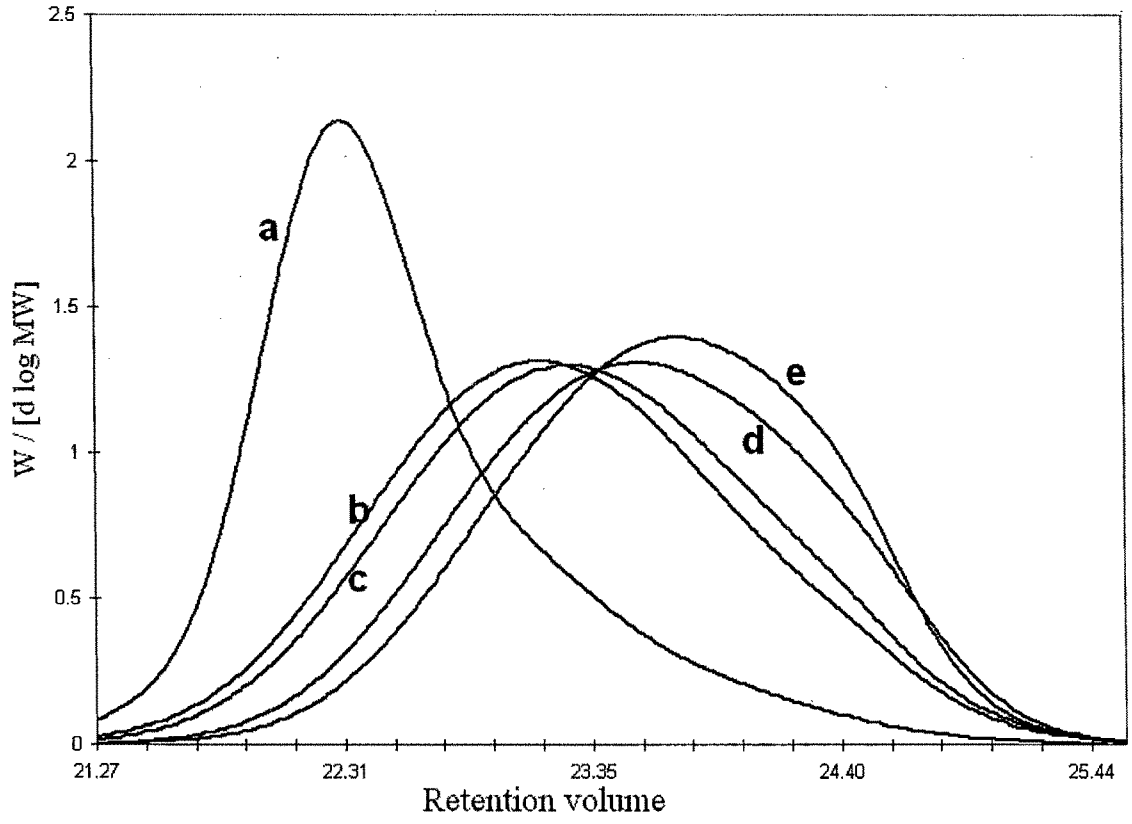

Fig. 3.19. GPC profile of polymer listed in Table 3.17, (a) commercial sample; (b) entry 1; (c) entry 2; (d) entry 3; (e) entry 4.

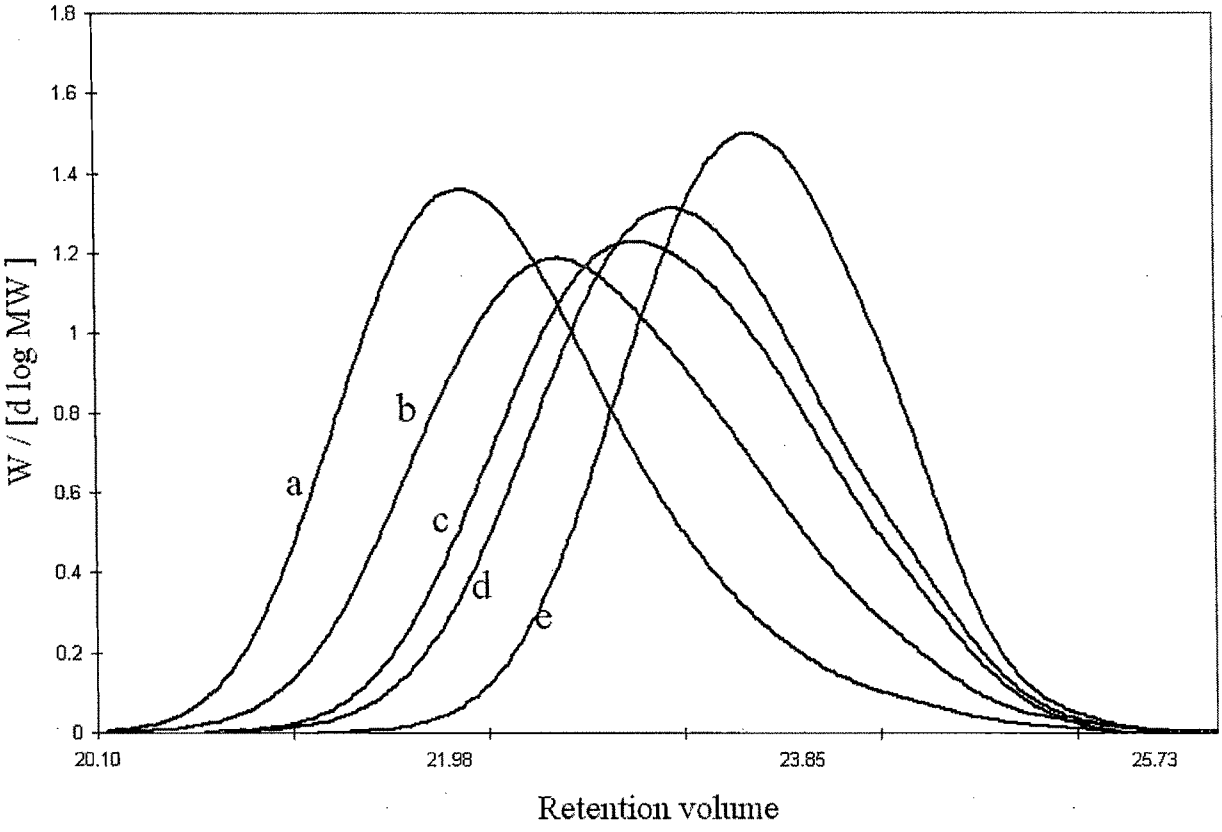

Fig. 3.20. GPC profile of polymer listed in Table 3.20, (a) entry 3; (b) entry 5; (c) entry 4; (d) entry 2; (e) entry1.

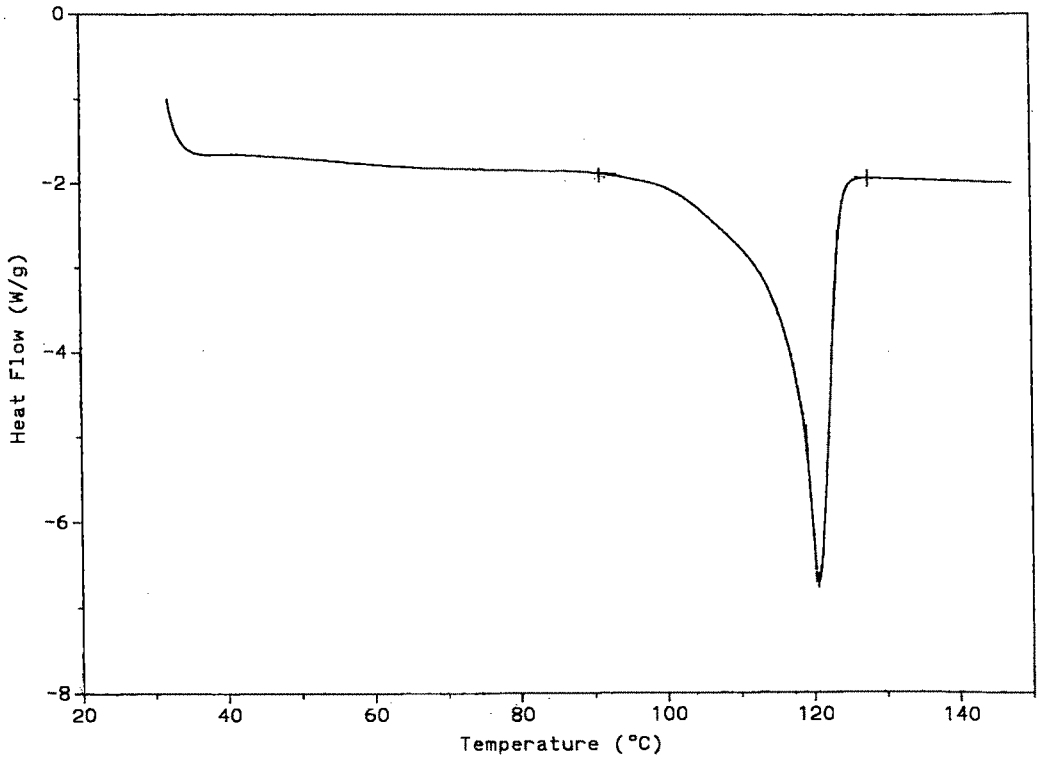

Fig. 3.21 DSC of PE wax, Table 3.17, entry 1.

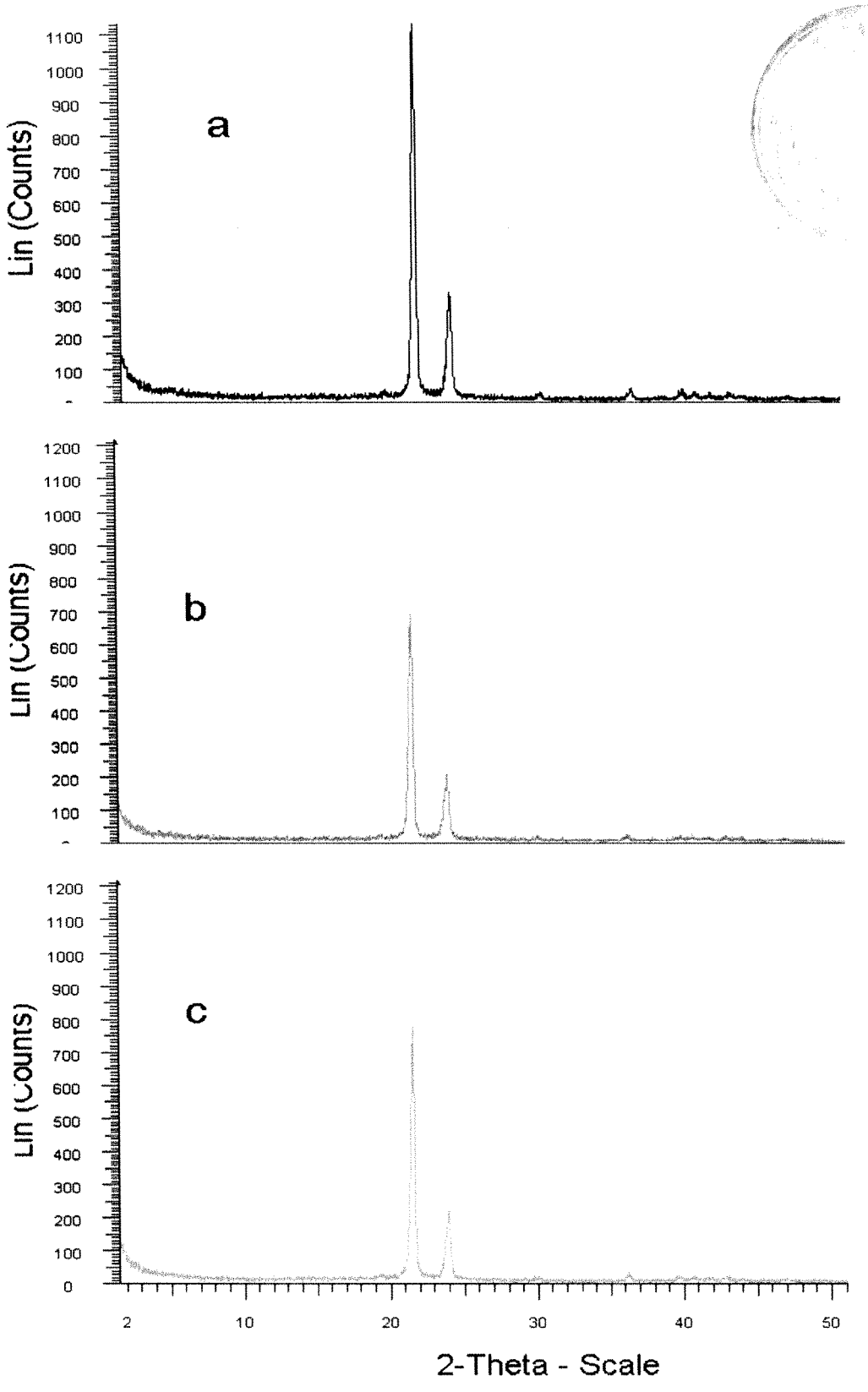

Fig. 3.22. XRD of PE wax, (a) Table 3.17, entry 1; (b) Table 3.17, entry 2; (c) and commercial sample.

3.5 $Ti(OR)_2(X)_2$, $Ti(OR)(OR')_2$ or $Ti(OR)_4$ Catalyst

In this section Titanium (IV) catalysts with sterically bulky phenolic ligands 2-*tert*-butyl-4 methylphenol, 2, 4 di-*tert*-butyl phenol and 3,5 di-*tert*- butyl phenol having empirical formula as $[Ti(OPh^*)_n(OPr^i)_{4-n}]$, ($OPh^*$ = substituted bulky phenol) have been synthesized and examined as catalyst in ethylene polymerization.

Synthesis of aryloxide complexes of Titanium

The preparation of Ti-phenolate complexes could be realized *via* stoichiometric reaction between $Ti(OPr^i)_4$ and the phenolic ligands (1:2 mole ratio in case of **21** and 1:4 mole ratio in case of **22–24**) and removal of liberated isopropanol azeotropically. The reaction in toluene afforded dark orange coloured complexes which were washed with warm toluene. The Titanium complexes **21-24** described by the empirical formulation $Ti(OPh^*)_n(OPr^i)_{4-n}$ are generally soluble in aromatic and chlorinated aromatic solvents.

Catalysts **21-24** have been characterized by microanalysis, IR, ^1H NMR, FAB mass spectra and thermal analysis.

Anal.calc. for

catalyst **21** ($C_{28}H_{44}O_4Ti$); C, 68.3; H, 9.0; Ti, 9.7; Found: C,68.2; H 8.8; Ti, 9.8;

catalyst **22** ($C_{44}H_{60}O_4Ti$); C, 75.4; H, 8.6; Ti, 6.8; Found: C,75.8; H 8.6; Ti, 6.9;

catalyst **23** ($C_{56}H_{84}O_4Ti$); C, 77.4; H, 9.7; Ti, 5.5; Found: C,77.8; H 10.1; Ti, 5.5;

catalyst **24** ($C_{56}H_{84}O_4Ti$); C, 77.4; H, 9.7; Ti, 5.5; Found: C,77.5; H 9.8; Ti, 5.8.

In a typical IR spectra of **21** the low intensity broad peaks in the 3000-3500 cm^{-1} region indicate the deprotonation of the phenolate ligand on complexation to titanium center.

In the ^1H NMR spectra (Fig. 3.23) a set of multiplets in the region 7.0 - 7.3 ppm for the aromatic protons was a noted in addition to signals due to methyl proton at 2.36 ppm and tertiary butyl group {-$C(CH_3)_3$} at 1.3 ppm.

In the FAB mass spectra of **23** a prominent peak for ligand fragment (phenolate ion) appears at 206. However, the parent ion was again not detected.

All the catalysts are quite stable as is apparent from the thermal degradation profile which indicates degradation peaks in the 200 to 400^0 C region. However, complete degradation to the dioxide, TiO_2 was observed beyond 480°C. Typical TG results for **21** (obs. 16.8 %; cal. 16.2 %) and **23** (obs. 8.9 %; cal. 9.2 %) support the solid state stoichiometry of the complexes inferred from microanalysis.

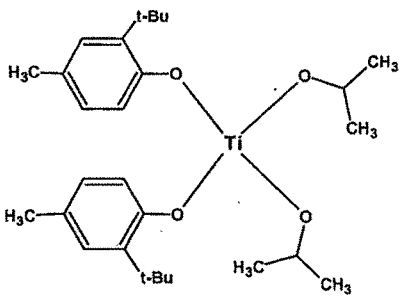

21

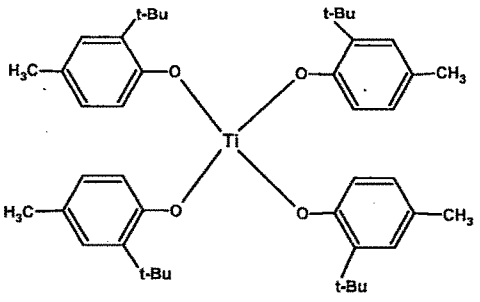

22

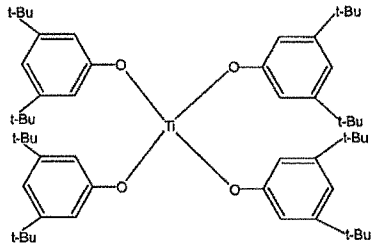

23

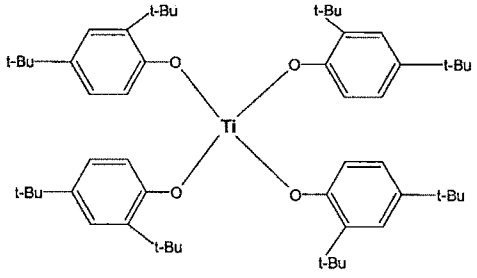

24

Scheme 3.8 Catalyst structure **21-23**

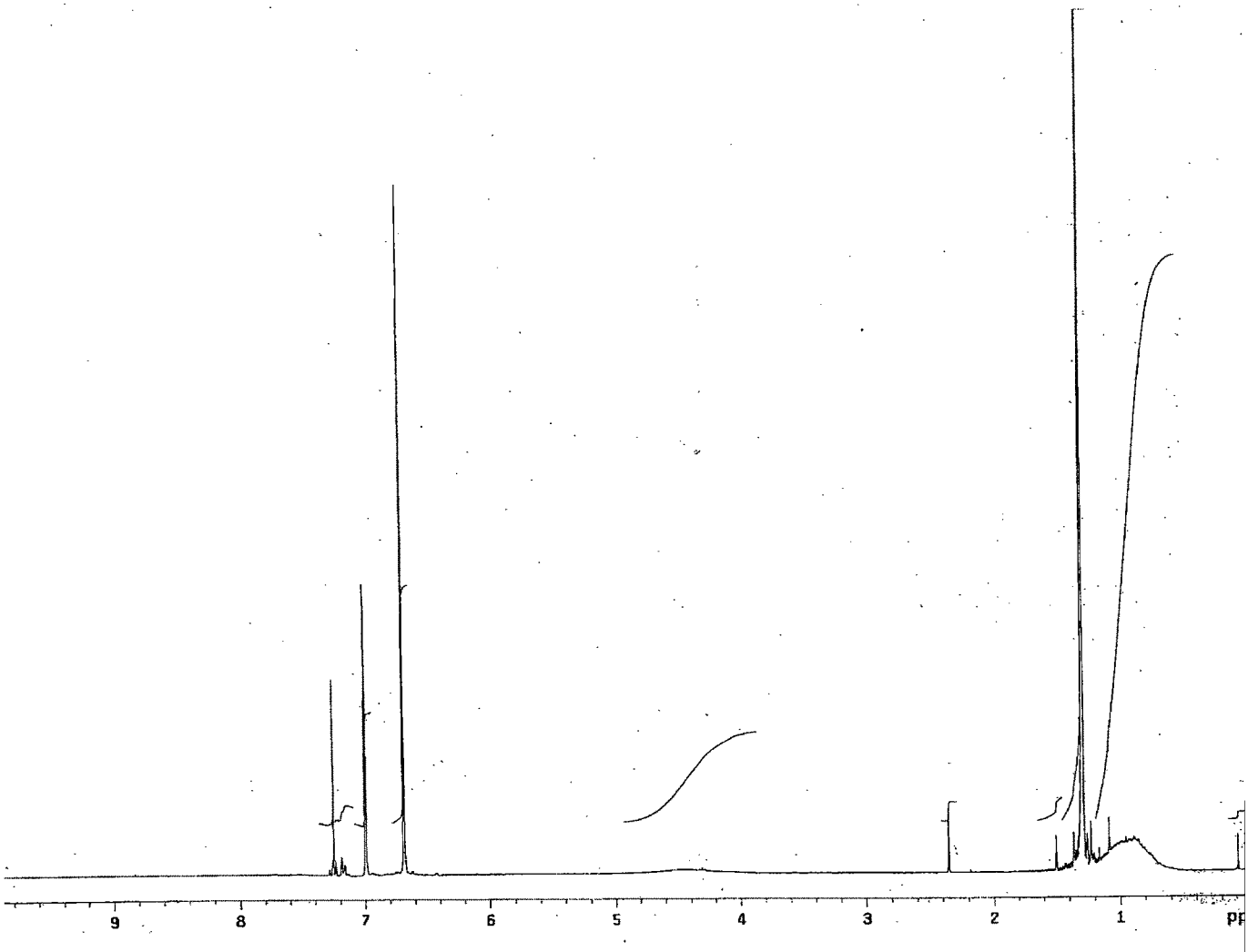

Fig. 3.23 ^{1}H NMR of catalyst **21**

Polymerization of Ethylene

The results of ethylene polymerization using catalyst precursors **21-24** are shown in Table 3.22. Evaluation of catalysts indicate that 1:2 titanium complex of 2-*tert*-butyl-4 methylphenol **(22)** shows higher activity (25 Kg PE/g Ti) than the 1:1 complex (20 Kg PE/g Ti). Replacement of the methyl group at 4 position with the *tert*- butyl group decreases the productivity dramatically. When the position of *tert*- butyl group is changed from 2, 4 position to 3, 5 position a slight increase in the productivity was observed. Molecular weights of the obtained polymer were observed to follow a similar trend as in the productivity.

Use of Ethylaluminum sesquichloride shows the highest productivity amongst all co-catalyst. $EtAlCl_2$ (EADC) (Table 3.22, entry 11) is also active but show lower productivities. Non-halogenated co-catalysts, methyl alumoxane (MAO) and triethylaluminum (TEAL, Et_3Al) (entry 10 & 12) display very less activity. Molecular weight of the polymer show M_w = 840 to 1290 and molecular weight distribution (M_w / M_n = 1.4-1.5). Increase in the reaction temperature (entry 3, 8 and 9) and pressure (entry 3 and 7) resulted increase in the productivity. Changeover of non polar solvent toluene to a polar solvent chlorobenzene showed nearly 25 % increase in productivity of polyethylene against the polymerization in aliphatic solvent like hexane.

The branching degree of PE's was determined from IR by taking the value of absorbance of 1378 cm^{-1} peak (νs CH_3) which was found to be 1.9. These values are consistent with generally fewer short chain branches (SCB) observed for most linear high density

polyethylenes (~1-2 /1000 C). Some representative GPC, DSC and XRD are illustrated in Figs. 3.24 to 3.26.

Table 3.22 Results of Ethylene polymerization with Ti-phenolate catalytic system [a]

Entry	Catalyst	Temp ° C	Pressure psi	Co Catalyst	Activity Kg PE/g Ti	M_w	PD	T_m °C	d(g/cc)
1	**21**	100	500	EASC	19.9	1290	1.5	118	0.952
2	**22**	100	500	EASC	24.7	1170	1.5	124	0.954
3	**23**	100	500	EASC	18.5	930	1.4	128	0.958
4	**24**	100	500	EASC	4.7	840	1.4	125	0.954
5	Cp_2TiCl_2	100	500	EASC	0.2	--	--	--	--
6	Cp_2ZrCl_2	100	500	EASC	1.0	--	--	--	--
7[b]	**22**	100	250	EASC	9.5	--	--	116	--
8[c]	**23**	50	500	EASC	2.6	--	--	--	--
9[d]	**23**	30	500	EASC	0.3	--	--	--	--
10	**23**	100	500	MAO	1.5	--	--	132	--
11	**23**	100	500	EADC	4.2	--	--	123	--
12	**23**	100	500	TEAL	0.2	--	--	--	--
13[e]	**23**	100	500	EASC	23.5	--	--	116	--
14[f]	**23**	100	500	EASC	0.1	--	--	--	--

[a]All reactions were carried out in a 600 mL SS reactor at 100°C and 500 psi ethylene pressure for 1h. in toluene.

[b](C_2H_4) = 250 psi ; Temp = 50°C [c], 30°C[d] ; Solvent = Chlorobenzene[e], Hexane[f].

EADC = $EtAlCl_2$, TEAL = Et_3Al

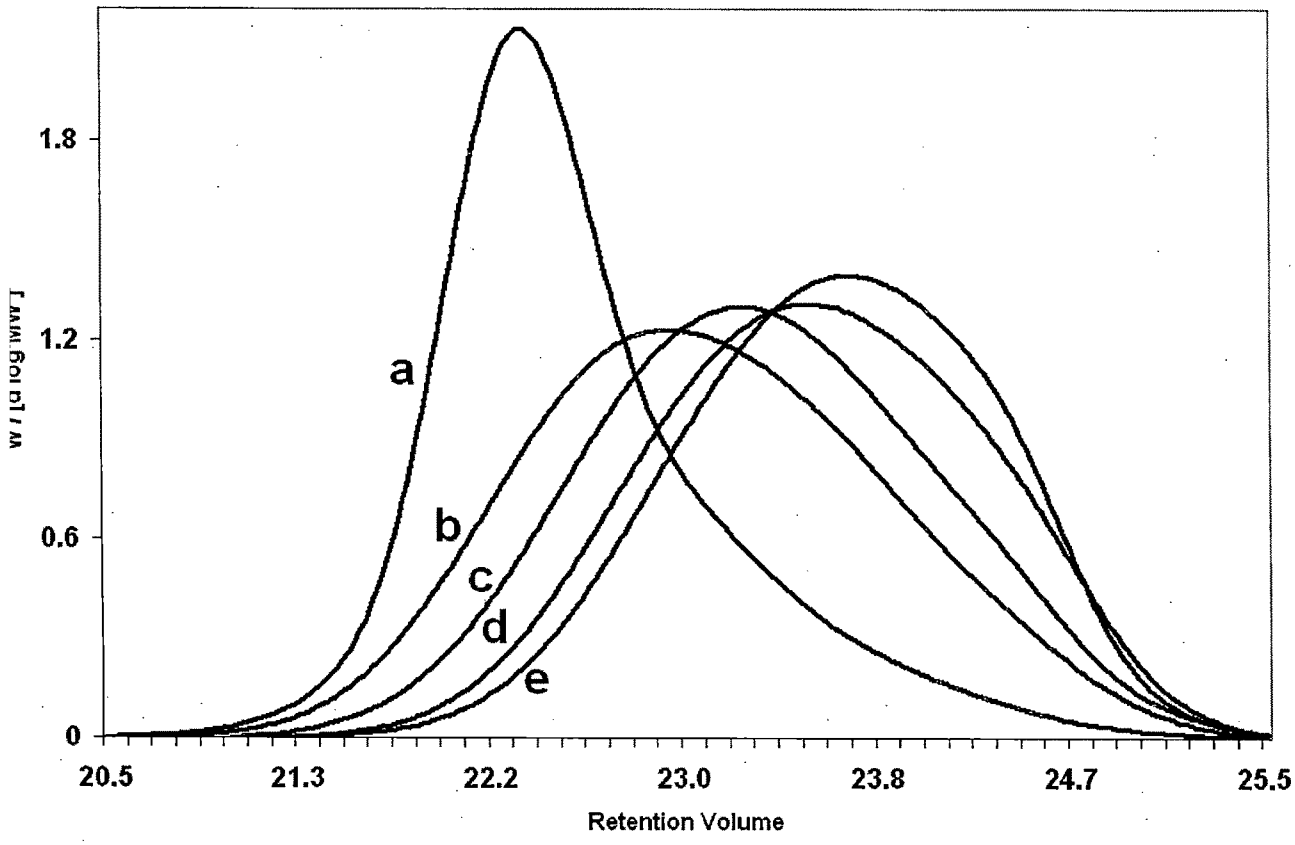

Fig. 3.24 GPC profile of polymer listed in Table 3.22 a) commercial sample, b) entry 1, c) entry 2, d) entry 3, e) entry 4.

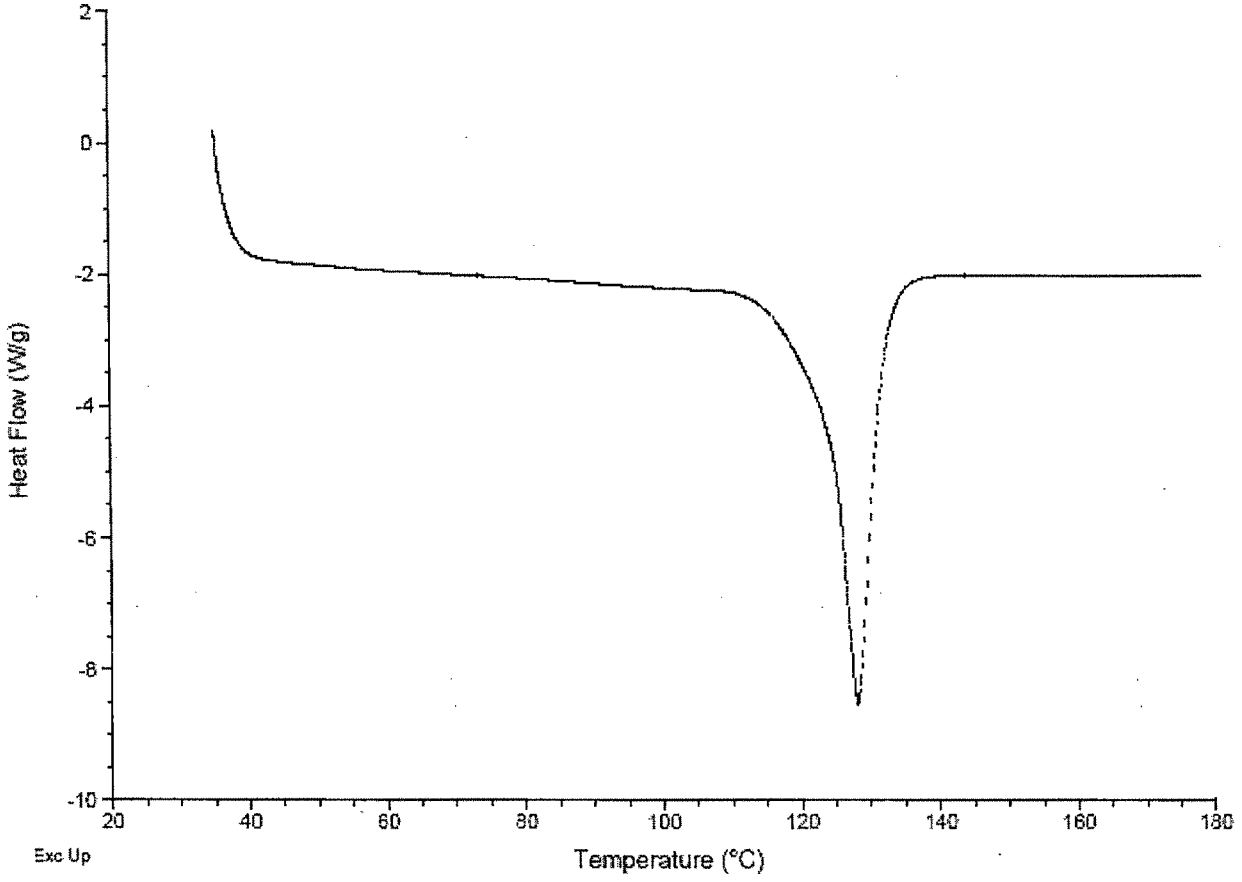

Fig. 3.25 DSC of PE wax Table 3.22 entry 2

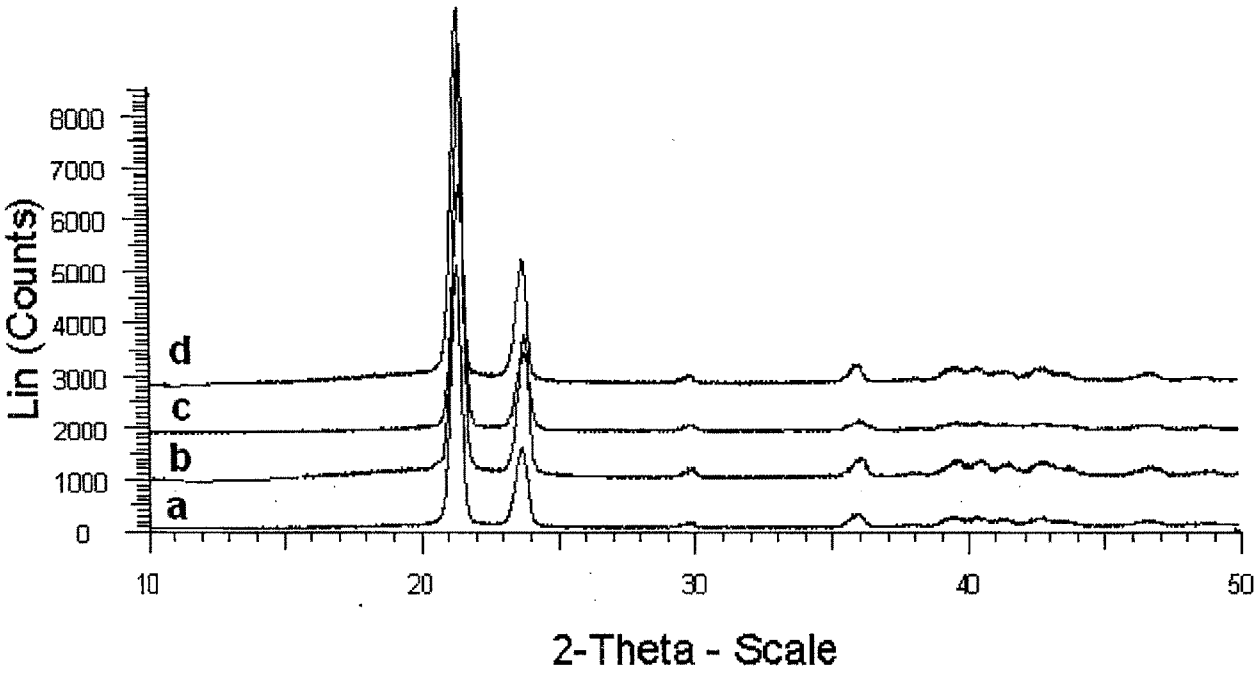

Fig. 3.26. XRD of PE wax Table 3.22 a) entry 1 b) entry 2 c) entry 3 d) entry 4

3.6 Hetero atom linked $[(RO)_3Ti(O\hat{}O)\ Ti(OR)_3]_n$ catalysts.

A series of novel Titanium (IV) complexes with S-bridged biphenol, 5-*tert*-butyl-4-hydroxy-2-methyl phenyl sulphide (BHMPS) formulated as $[(RO)_3Ti\ (O\hat{}O)\ Ti(OR)_3]_n$ were prepared starting from different $Ti(OR)_4$ precursors (R = ethyl, *i*-propyl, *i*-butyl and chloride). These catalysts (**25-28**) were studied for polymerization of ethylene.

Preparation of catalysts

To a solution of 2 mmol of $Ti(OR)_4$ in toluene (25 mL) was added slowly 1 mmol of BHMPS in toluene (30 mL) under nitrogen atmosphere and heated at 60°C for 3 hr. The contents were then stirred for 24 hr at room temperature. Evaporation of solvent and volatiles yielded reddish-yellow coloured powders that were isolated by filtration, dried under vacuum and used further in ethylene polymerization.

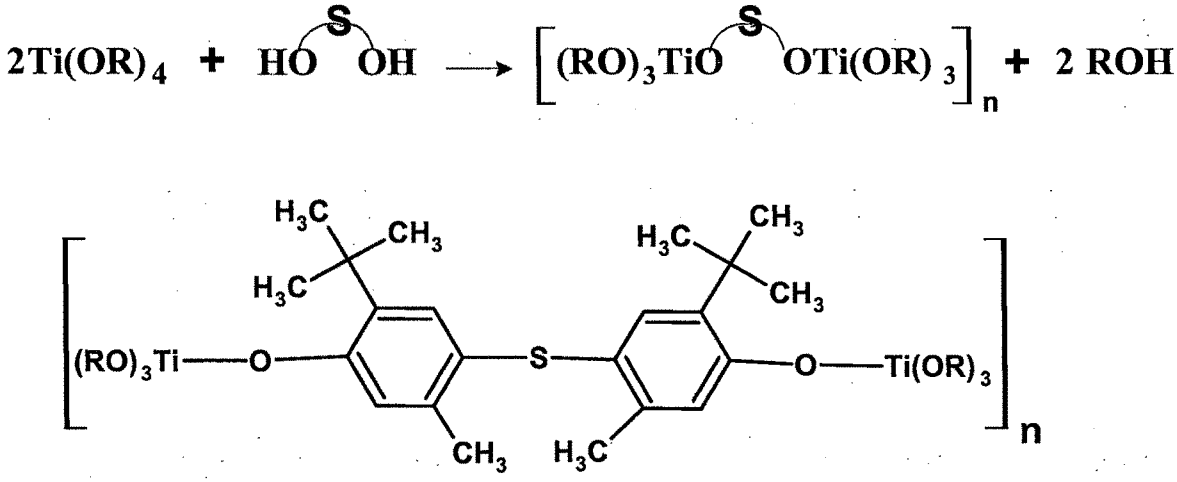

R = C_2H_5 [**25**], R =, *i*-C_3H_7 [**26**], R = *i*-C_4H_{11} [**27**], R = Cl [**28**]

Scheme 3.9. Synthesis of catalyst **25-28**

The catalyts **25-28** shown in Scheme 3.8 have been characterized by IR, elemental and thermo gravimetric analysis. Low solubility of complexes in common organic solvents at room temperature precluded NMR spectral characterization. The IR spectra of **25-28** indicate the absence of νOH peak (~ 3000-3200 cm^{-1}) of starting BHMPS suggesting complete exchange by –OR groups. However, the insoluble nature of all these Ti-catalysts indicates the possibility of formation of linear aggregates limiting further characterization of these solids.

Ethylene Polymerization

The results of ethylene polymerization by Ti - complexes **25- 28** are compiled in Table 3.23. To our surprise all the Ti-complexes display high activity. This can possibly be explained by the fact that under the influence of Al-alkyl co-catalyst & at higher temperature active species will be generated by cleavage of ~ [Ti-OR-Ti] ~ linkages in the initially isolated polynuclear solid complexes. The S-bridge between the two phenolic groups presumably impart strong influence on the overall catalytic performance. This, however, would require further confirmation from structure-activity studies. In contrast to the soluble Ti-biphenolate systems the BHMPS-based Ti- catalyst induce polymerization as a suspension in toluene at higher temperature.

At lower temperatures PE productivity is considerably reduced from 17 to 0.5 Kg PE/g Ti (Table 3.23, entry 1 & 11) and the polymer display broad melting peaks. Similarly an increase in ethylene pressure to 500 psi also results in nearly two fold increase in activity from 7.2 to 17 Kg PE/ g Ti (Table 3.23, entry 1 & 12).

Halogenated co-catalysts EASC has demonstrated highest productivity (17 Kg PE/g Ti) where as the non-halogenated alkylaluminums like Et_3Al and MAO are inactive (Table 3.23, entry 5-8). Use of chlorobenzene as a solvent results in significant increase in productivity to 22.5 Kg PE/ g Ti (Table 3.23, entry 1 & 9) with consequent reduction in molecular weight from 1800 to 800.

Gel Permeation Chromatographic (Fig. 3.28) results indicate low-molecular weights for these polymers ($M_w < 3000$) and narrow dispersities ($M_w / M_n = 1.3\text{-}1.9$) accompanied by higher X_c (72-81 %) as computed from specific heat of fusion in DSC (Fig. 3.27). The crystalline nature was also supported by XRD (Fig. 3.29). The melt temperatures are in the range of 110^0–128^0C. The polymer particles appear as well separated crystalline blocks having sharp plate like features, as seen by Scanning Electron Micrograph. (Fig. 3.30)

Table 3.23 Ethylene Polymerization by Ti(IV) - BHMPS – Alkyl aluminum catalysts

Entry	Cat.	Co cat.	Al : Ti ratio	$^{P}C_2H_4$ psi	T °C	Productivity Kg PE / g Ti	M_w	PDI	T_m °C
1	**25**	EASC	300	500	100	17	1800	1.5	115
2	**26**	EASC	300	500	100	14.5	3200	1.9	123
3	**27**	EASC	300	500	100	13.6	1320	1.5	119
4	**28**	EASC	300	500	100	2.1	1860	1.7	122
5	**25**	DEAC[c]	300	500	100	3.5	--	--	128
6	**25**	TEAL[c]	300	500	100	0.9	--	--	--
7	**25**	EADC[c]	300	500	100	1.2	--	--	--
8	**25**	MAO	300	500	100	0.1	--	--	--
9[b]	**25**	EASC	300	500	100	22.5	800	1.3	110
10	**25**	EASC	300	500	50	3.8	--	--	123
11	**25**	EASC	300	500	RT	0.5	--	--	--
12	**25**	EASC	300	200	100	7.2	--	--	--
13	**25**	EASC	500	500	100	25.8	--	--	--
14	**25**	EASC	50	500	100	0.3	--	--	--

[a] All reactions were carried out in a 600 mL SS reactor for 1h in toluene..

[b] Solvent chlorobenzene.

[c]DEAC = Et_2AlCl, EADC = $EtAlCl_2$, TEAL = Et_3Al.

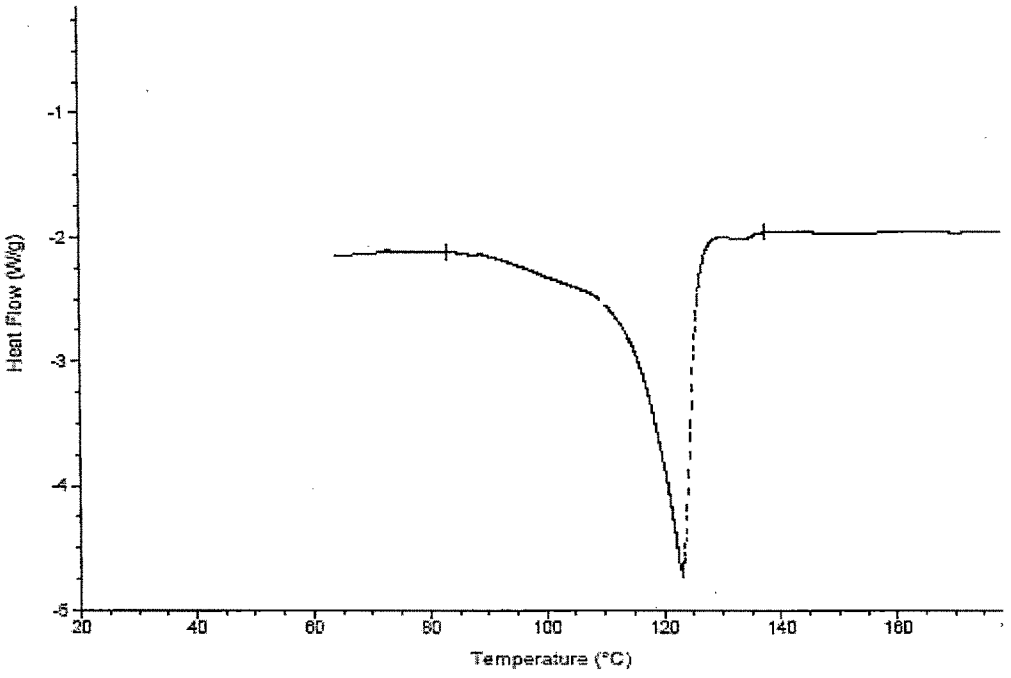

Fig. 3.27. Representative DSC of PE wax entry 2, Table 3.23

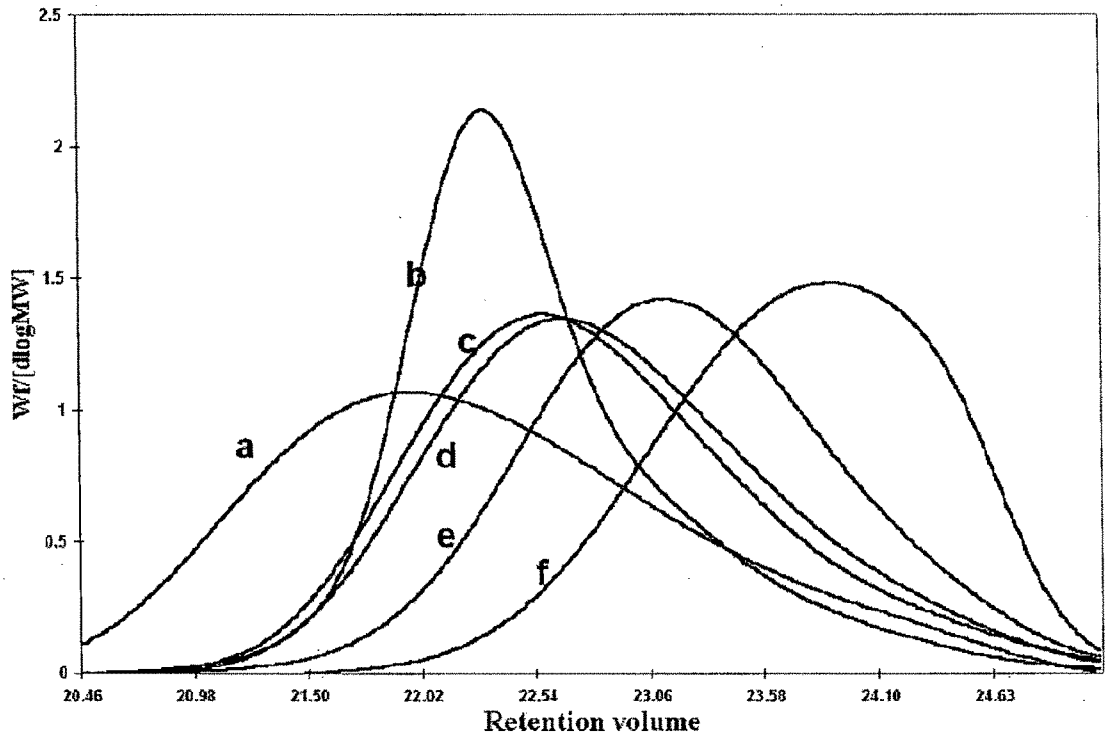

Fig. 3.28. GPC profile of polymer listed in Table 3.23 a) entry 2, b) commercial sample , c) entry 4, d) entry 1, e) entry 3, f) entry 9.

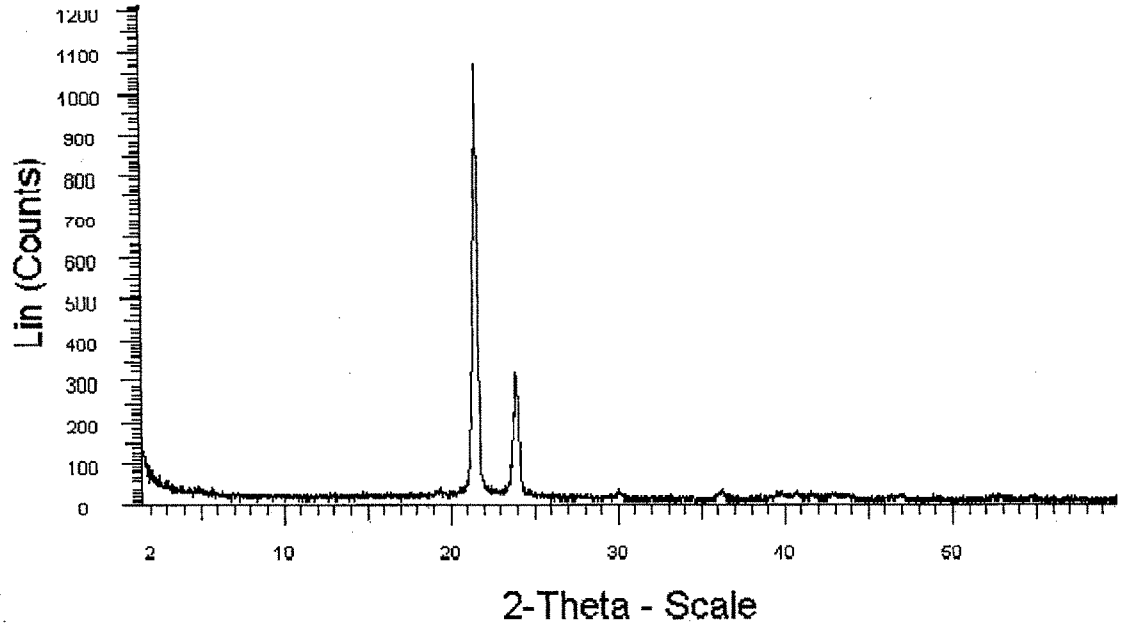

Fig. 3.29. XRD of PE wax (Table 3.23, entry 1).

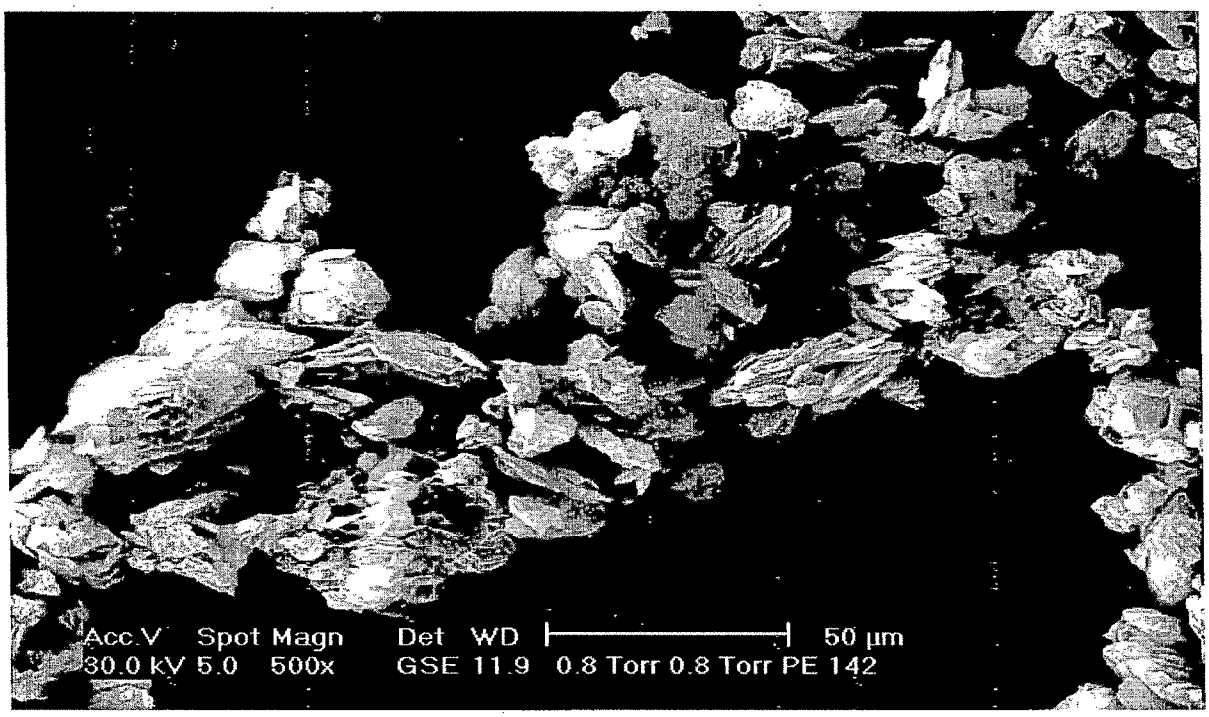

Fig. 3.30. SEM of PE wax (Table 3.29, entry 1)

3.7 MECHANISM

Introduction

In this section, the possible mechanistic aspect concerning the catalytic activity of Titanium-aryloxides in ethylene polymerization has been delineated.

Catalytic precursor

Treatment of mononuclear $Ti(OR)_4$ type alkoxides with alkylaluminum halides has been reported to yield active intermediates (shown below) responsible for the polymerization of ethylene to low molecular weight products [19, 20].

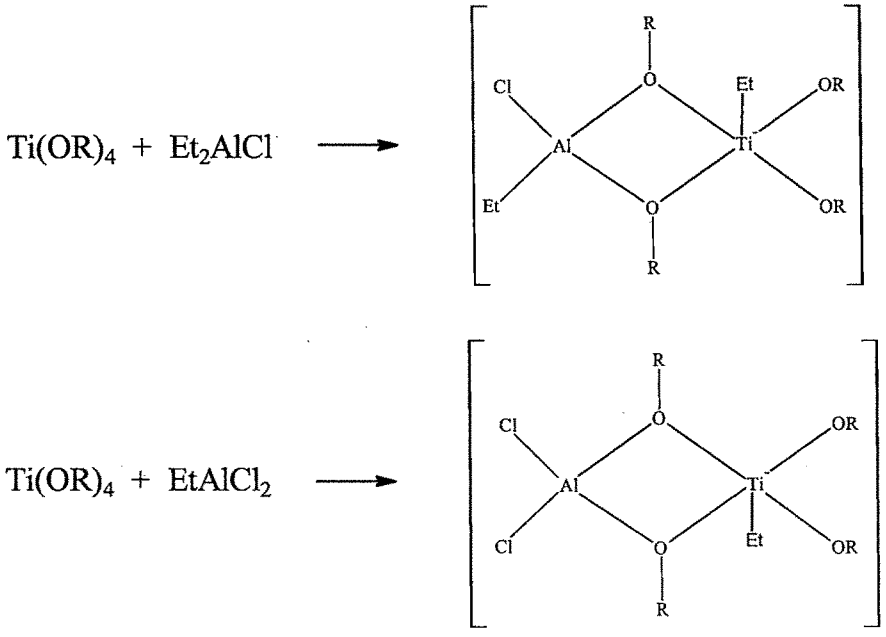

Scheme 3.10. Active intermediate for polymerization

We believe that similar type of active species may be involved in the present Ti-biphenolate system. Moreover, as EASC is derived from an equimolar mixture of EADC and DEAC [21], we have

$$2\ Et_3Al_2Cl_3 \rightleftharpoons (EtAlCl_2)_2 + (Et_2AlCl)_2$$

Further since EASC dissociates as Et_2AlCl and $EtAlCl_2$ in solution it is reasonable to expect the formation of two type of catalytic species on interaction with Ti - biphenolate catalyst. The reduction of Ti(IV) in presence of EASC will generate catalytically active components.

Qualitative information on the course of reaction was followed with the help of UV-VIS spectrum at different stages of mixing of catalyst precursor & EASC in toluene. For eg. in Fig. 3.31 the peak at 365 nm after immediate addition of EASC to $Ti(O\text{-}O)(OPr^i)_2$ disappears (intensity is reduced). The introduction of ethylene leads to a new peak at around 460 nm (LMCT band). A similar evidence for the formation of active Ti-alkyl species was proposed for ethylene polymerization using a metallocene, Cp_2TiCl_2 and MAO by Kaminsky and others [22].

As shown in Scheme 3.10, the active catalysts in polymerization need to retain monomeric four or five coordinate geometry to allow olefin insertion and subsequent propagation [23]. In the present Ti -biphenolate catalytic system higher temperatures tend to favour formation of active intermediates responsible for polymerization.

Reaction Pathway

It is now well established that unoccupied coordination site and Ti-alkyl bond in the titanium complex are fundamental requirements for its polymerization activity. From the foregoing discussion it follows that, for the different Ti-catalyst precursors examined in this study the activities and molecular weight dependence is primarily governed by i) size and linkage of aryloxy group ii) type of alkyl aluminum co-catalyst and finally iii) reaction conditions of polymerization.

Two of the widely accepted mechanisms concerning active centers in Z-N polymerization consist of a bimetallic system in which Ti is bonded to Al through halide or halide-alkyl bridge or of monometallic system where only a titanium ion is the catalytic center. Based on a theoretical study by Morokuma [24] on the catalytic polymerization by chelating bridged and non-bridged Titanium aryloxides it is possible to predict the possible course of ethylene polymerization for the present Ti-biphenolate – EASC catalytic system. The active cationic species generated from the 'precatalyst' intermediates shown in Scheme 3.11 will facilitate the insertion of ethylene (rate determining step) into the growing chain which ultimately leads to the desired polyethylene *via* propagation and termination steps. Modified Novaro type mechanism [25, 26] can thus be extended to rationalize the polyethylene formation with these catalysts.

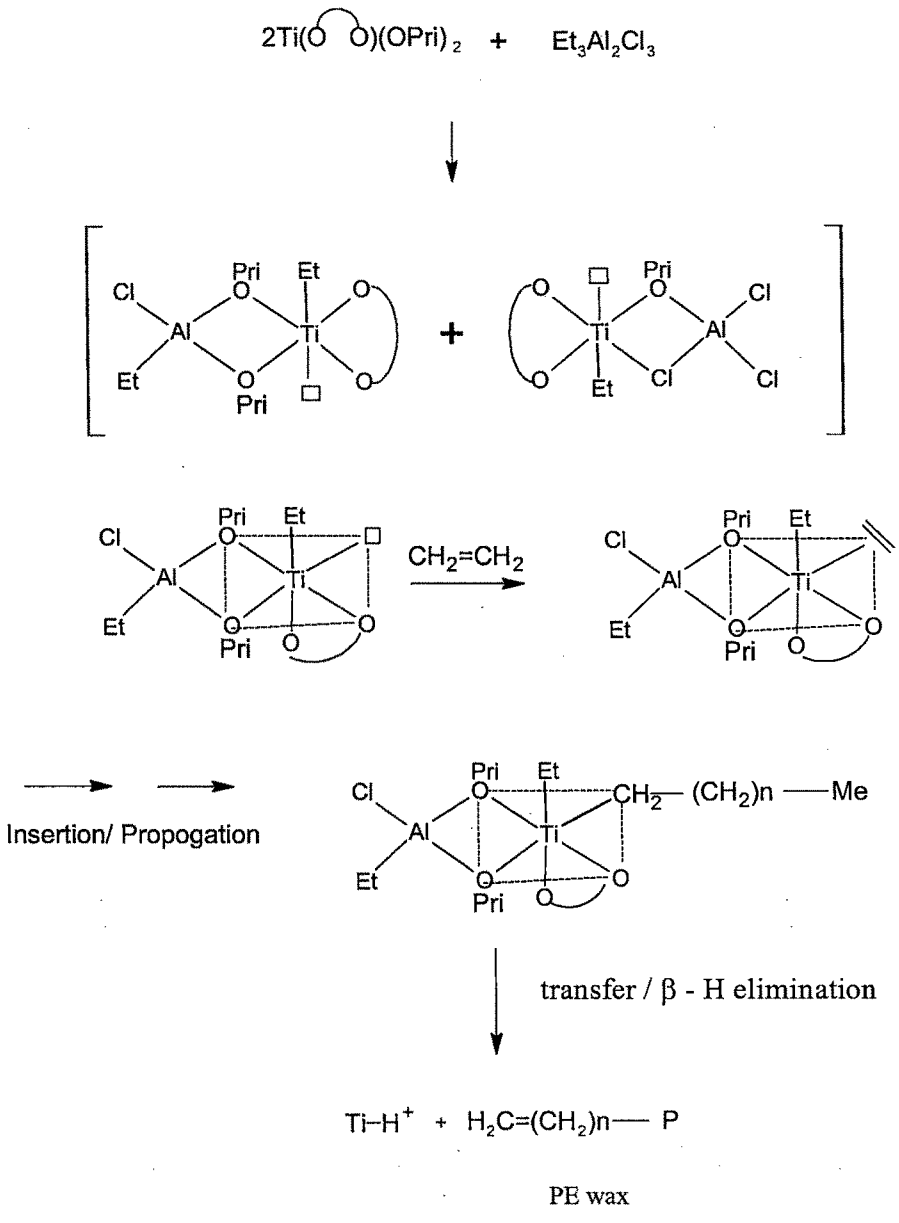

Scheme 3.11 Postulated mechanism of ethylene polymerization by catalyst and EASC.

The ethylaluminum sesquichloride plays a dual role. It exchanges the ligands with the Ti-ion there by forming labile Ti-alkyl bond and forms *via* the Al-O-Ti bridge adequate geometric structure & reduces Ti (IV) to Ti (III). Ethylene complexation causes the change of structure to an octahedra in which the monomer gets coordinated and successively inserted into the Ti-C bond leading to polyethylene wax with number of chains represented as $40 < n < 100$. Though chain transfer can occur by other reactions as well, however, the relative inactivity of these catalysts with MAO & Et_3Al indicates that termination is unlikely to proceed by transfer to Al-alkyl or by H_2 under the reaction conditions [27]. From this it follows that the steric bulk of chelated biphenol in the catalysts contributes in increasing the electron density around Ti ion and therefore inhibit co-oligomerization between higher alpha olefins. This essentially leads to linear polyethylene wax formation. Although the structure of active intermediates is as yet unknown the mechanism leading to these ultra low molecular weight PE waxes is consistent with those reported previously for solution phase olefin polymerization using titanium alkoxides and aluminum alkyls [24, 28]. Efforts are underway to investigate the detailed kinetics of this reaction.

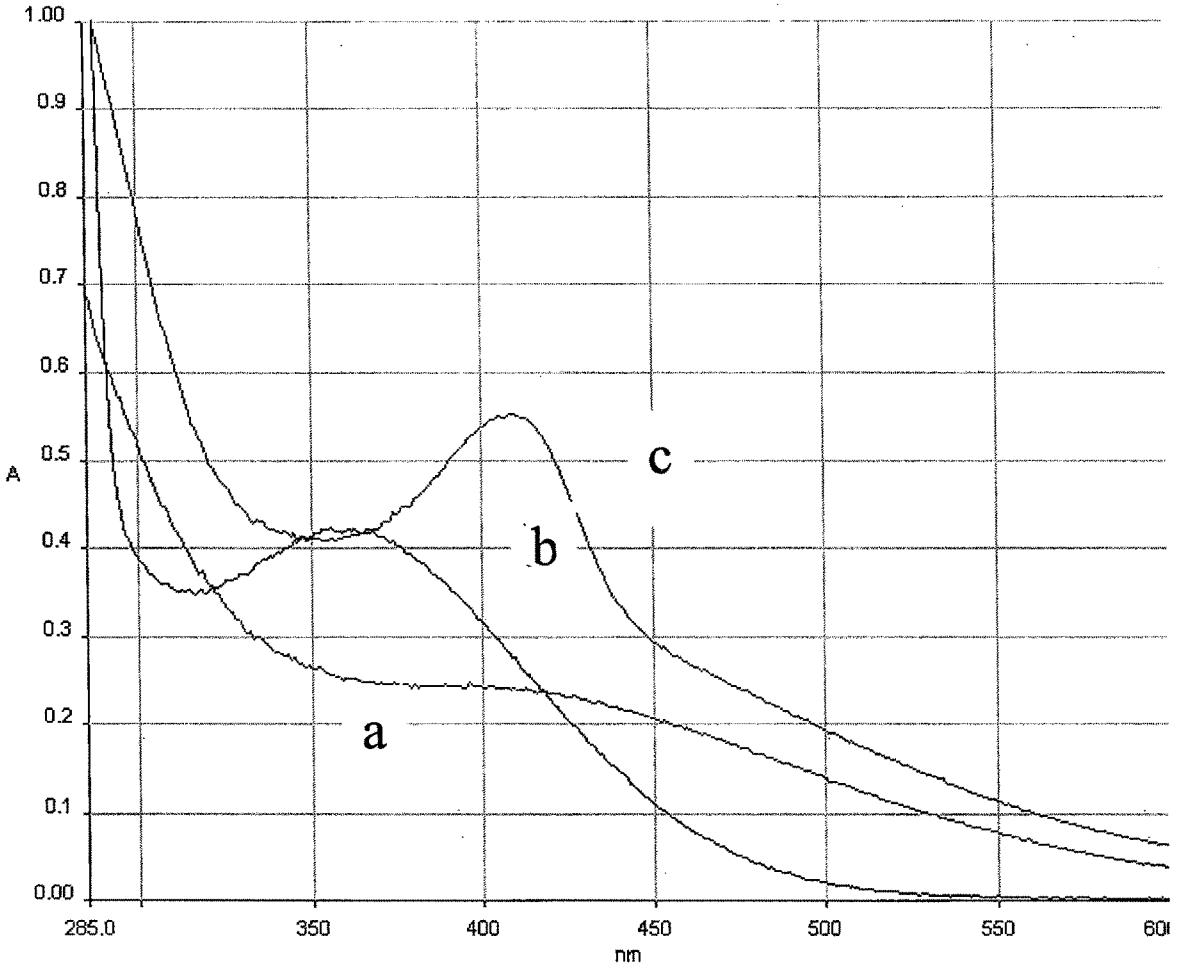

Fig. 3.31. UV spectrum a) Cat **1** + EASC , b) Cat **1** c) Cat **1** + EASC + C_2H_4

3.8 References

1) (a)T. J. Boyle, T. L. Barnes, J. A. Heppert, L. Morales, F. Takusagawa, *Organometallics*, 11 (1992) 1112; (b) G. Erker, S. Dehnicke, M. Rump, C. Krüger, S. Werner, M. Nolte, *Angew. Chem. Int. Ed. Engl.*, 30 (1991) 1349; (c) T. J. Boyle, N. W. Eilerts, J. A. Heppert, F. Takusagawa, *Organometallics*, 13 (1994) 2218; (d) M. Terada, Y. Matsumoto, Y. Nakamuza, K. Mikami, Inorg. *Chim. Acta.*, 296 (1999) 267; (e) J. A. Heppert, S. D. Dietz, T. J. Boyle, F. Takusagawa, *J. Am. Chem. Soc.*, 111 (1989) 1503; (f) N. W. Eilerts, J. A. Heppert, M. L. Kennedy, T. Takusagawa. *Inorg. Chem.*, 33 (1994) 4813; (g) N. W. Eilerts, J. A. Heppert, *Polyhedron,* 14 (1995) 3255.

2) (a) J. Balsells, T. J. Davis, P. Carroll, P. J. Walsh. *J. Am. Chem. Soc.,* 124 (2002) 10336; (b) T. J. Davis, J. Balsells, P. J. Carroll, P.J. P. J. Walsh, *Org. Lett.*, 3 (2001) 699; (c) J. Long, J. Hu, X. Shen, B. Ji, K. Ding *J. Am. Chem. Soc.*, 124 (2002) 10.

3) J. P. Corden, W. Errington, P. Moore, M. G. Partridge, M. G. H. Wallbridge, *J. Chem. Soc. Dalton Trans,* (2004) 1845.

4) (a) K. S. Andrä, *J. Organomet. Chem.*, 11 (1968) 567; (b) P. C. Wailes, R. S. P. Coults, H. Weigold, Organometallic Chemistry of Titanium, Zirconium and Hafnium ; Academic, New York, 1974 ; p.63.

5) M. G. Finn, K. B. Sharpless, *J. Am. Chem. Soc.*, 113 (1991) 113.

6) Based on a detailed solution and solid state studies of the reaction of 3,3'-disubstituted Binol derivatives with $Ti(OPr^i)_4$ monomeric $[(R_2\text{-Binol})Ti(OPr^i)_2]$

(R = $Si(Bu^t)Me_2$) and a heterochiral dimer in solution with bridging naphthoxy oxygens (R=Me) were reported when the ratio of the Ti-precursor & Binol was 1:1 (see Ref.14). On the other hand $(Me_2Binol)_2Ti$ was isolated by reacting $TiCl_4$ and Li_2(3,3' Me_2Binol) in the molar ratio of 1:2 This latter homoleptic complex was not characterized further. To date the solid state monomeric structure of $Ti(Binol)_2$ type complex has not been elucidated. Recently Walsh et.al (Ref. 15a, b) have characterized three new types of dimeric and trimeric binolate complexes while studying the interaction of Ti $(OPr^i)_4$ and Binol at higher molar ratio of 2 :1 and 6:1. No structural details on the solid state monomeric Ti(IV)-bis binolate was, however, available.

7) Given the facile nature of alkoxide groups to aggregate, the possibility of involvement of oligomeric complexes such as [Ti(Binolate) $(OPr^i)_2]_n$ in asymmetric synthesis has been ruled out indicating that the active catalytic species are necessarily different than the precursor in the solid state. a) M. Mori, T. Nakavi, *Tetrahedron Lett.* 38 (1997) 6233; b) P. J. Walsh, *Acct. Chem. Res.*, 36 (2003) 739; (c) C. Girard, H. B. Kagan, *Angew. Chem. Int. Ed.*, 37 (1998) 2922.

8) (a) X. Y. E. Chen, T. J. Marks, *Chem. Rev.*, 100 (2000) 1391; (b) P. A. Deck, T. J. Marks, *J. Am. Chem. Soc.*, 117 (1995) 6128.

9) A. K. Rappe, W. M. Skiff, C. J. Casewit, *Chem. Rev.*, 100 (2000) 1435.

10) Y. Nakayama, K. Miyamoto, N. Ueyama, A. Nakamura, *Chem. Lett.*, (1999) 391.

11) The commercial sample employed in this work, MPP 635 is a micronized, high melt point, crystalline form of polyethylene which was supplied by M/s Micro

Powders, Inc. USA. The product has a T_m of 123-125 ^{0}C, mol.wt. 2000, d (25^{0}C) 0.96 and max. particle size = 31 microns. These and other grades of polyethylene waxes have been designed to increase the abrasion resistance and anti-blocking characteristics in flexographic inks as well as industrial paints and coatings. More details at www.micropowders.com.

12) G. Dlubek, Th. Lupke, J. Stejny, M. A. Alam, M. Arnold, *Macromolecules,* 33 (2000) 990.

13) K. Gigant, A. Rammal, M. Henry, *J Am Chem Soc.*, 123 (2001) 11632.

14) R. O. Duthaler, A. Hafner, *Chem. Rev.,* 92 (1992) 807.

15) a) M. Mori, T. Nakavi, *Tetrahedron Lett.,* 38 (1997) 6233; b) P. J. Walsh, *Acct. Chem. Res.,* 36 (2003) 739; (c) C. Girard, H. B. Kagan, *Angew Chem. Int. Ed. Engl.,* 37, (1998) 2922.

16) (a) M. Lorca, D. Kuhn, M. Kurosu, *Tetrahedron Lett.,* 42 (2001) 6243; (b) S. Kobayashi, K. Kusakabe, S. Komiyama, H. Ishitani, *J. Org. Chem.,* 64 (1999) 4220; (c) K. Mikami, T. Korenaga, Y. Matsumoto, M. Veki, M. Terada, M., S. Matsukawa, *Pure Appl. Chem.,* 73 (2001) 255; (d) Y. Yamashita, H. Ishitani, H. Shimizy, S. Kobayashi, *J. Am. Chem. Soc.,* 124 (2002) 3292.

17) (a) T. J. Davis, P. J. Caroll, P. J. Walsh, *J. Organomet. Chem.,* 663 (2002) 70; (b) Y. Takashima, Y. Nakayama, K. Watanaba, T. Itono, N. Ueyama, A. Nakama, H. Yasuda, A. Harada, *Macromolecules,* 35 (2002) 7538; (c) D. Takeuchi, Y. Watanabe, T. Aida, S. Inoue, *Macromolecules,* 28 (1995) 651; (d) D. Takeuchi, T. Nakamusa, T. Aida, *Macromolecules,* 33 (2000) 725; (e) D. Takeuchi, T.

Aida, *Macromolecules,* 33 (2000) 4607; (f) M. H. Chishlom, J. H. Huang, J. C. Huffman, E. E. Streib, D. Tiedtke, *Polyhedron,* 16 (1997) 2941.

18) A. N. Penin, T. A. Sukhova, N. M. Bravaya. *J. Poly. Sci. A Poly. Chem.*, 39 (2001) 1901.

19) (a) H. Hirai, K. Hiraki, I. Noguchi, S. Makishima, *J. Poly. Sci., Part A* 8 (1970) 47 (b) A. E. Shilov, T. S. Dzhabiev, R. D. Sabirova, *Kinet. Catal., Engl. Transl.,* 5 (1964) 385. (c) P. H. Moyer, *J. Poly. Sci. A*, 3 (1965) 199. (d) E. Angelescu, C. Nicolau, Z. Simon, *J. Am. Chem. Soc.,* 88 (1966) 3910.

20) R. A. Rothenburg, *J. Poly. Sci.* A, 3 (1965) 3038.

21) W. Kaminsky in (transition metal catalyzed polymerizations – Alkenes and Dienes, Hardward academic NW (1981). p. 233.

22) (a) T. Mole, E. A. Jeffery, Organoaluminum compounds; Elsevier : New York 1972 p.9 (b) J. Brandt, E. G. Hoffman, *Brennstoff-Chem.*, 45 (1962) 200.

23) G. H. Olivé, S. Olivé, *Coordination and Catalysis*, Verlag chemie, Weinheim, NY, 1977, P 193.

24) (a) R. D. J. Froese, D. G. Musaev, T. Matsubara, K. Morokuma, *J. Am. Chem. Soc.*,119 (1997) 7190; (b) R. D. J. Froese, D. G. Musaev, T. Matsubara, K. Morokuma, *Organometallics*, 18 (1999) 373.

25) O. Novaro, S. Chaw, P Magnaut, *J. Catal*, 41 (1976) 91.

26) K. S. Minsker, M. M. Karpassas, J. V. Zaikov, *J. Macromol. Sci. Rev. Macromol. Chem. Phy.*, (1987) C-27, 1.

27) (a) F. G. Sernetz, R. Mulhaupt , S. Fokken, J. Okuda, *Macromolecules,* 30 (1997) 1562; (b) C. Capacchione, A. Proto, H. Ebeling, R. Mülhaupt, K. Möller, R. Manivannan, T. P. Spaniol, J. Okuda, *J. Mol. Catal. A Chemical,* 213 (2004) 137.

28) (a) K. Watenpaugh, C. N. Caughlan, *Inorg. Chem.*, 5 (1966) 1782; (b) M. J. Frazer, Z. Goffer, *J. Inorg. Nucl. Chem.*, 28 (1966) 2410.